The effects of public health measures on severe dengue cases: an optimal control approach

Akhil Kumar Srivastav[a], Vanessa Steindorf[a], Nico Stollenwerk[a] and Maíra Aguiar[a,b,c,*]

[a]Basque Center for Applied Mathematics - BCAM, Mazzaredo 14, Bilbao, 48009, Spain
[b]Ikerbasque, Basque Foundation for Science, Euskadi Plaza, 5, Bilbao, 48009, Bizkaia, Spain
[c]Dipartimento di Matematica, Universita degli Studi di Trento, Via Sommarive, 14, Trento, 38123, Italy

ARTICLE INFO

Keywords:
optimal control
vector-host model
vaccination
dengue fever
cross temporary immunity
ADE

ABSTRACT

Dengue fever is the most important viral mosquito-borne disease worldwide, with approximately 3.9 billion people at risk of acquiring dengue infection. Measures against mosquito bite combined with vector control programs to reduce mosquito population have been used in endemic countries for several years. Most recently, vaccines have become an important ally to prevent and control disease transmission. Economic costs of dengue control programs vary from region to region and therefore designing an optimal control strategy must be evaluated at different epidemiological contexts. Using a multi-strain vector-host mathematical model, we investigate the impact of different control measures to reduce dengue prevalence. A detailed sensitivity analysis to identify the key parameters influencing disease transmission is followed by an exploratory analysis of the possible solutions for the optimal control problem considering preventive measures to avoid mosquito bites, reduce mosquito population and vaccinate human hosts. The proposed cost functional includes a weighted sum of several efforts (not necessarily quantified as economic costs) for the controls which are evaluated alone and combined. The control system is analyzed using the Pontryagin's Principle for optimal control where different strategies are compared. Our results have shown that the simultaneous use of intervention measures are highly effective to reduce disease cases, however, the use of a single control measure can be as effective as the use of two or more controls combined. A careful evaluation of the epidemiological scenario is advised before designing strategies for disease prevention and control, allowing an optimal allocation of the public health resources.

1. Introduction

Mathematical modeling plays an important role in predicting new disease cases, assessing risks and evaluating the impact of the various control measures implemented during an outbreak. While the dynamics of infectious diseases are by nature non-linear, the understanding of such non-linear processes is vital, both for medical and economic reasons. Optimal control theory is often used to investigate the effect of intervention measures implementation in the context of public health [1–3], with the Pontryagin's Principle being used by several authors to evaluate the performance of vaccination and medical treatment, for example. In this paper, we evaluate the impact of the available public health measures used in endemic countries to control the spread of dengue fever. Differently from the already existing models, we investigate a multi-strain vector-host framework that includes the combination of two biological features of dengue fever epidemiology generating complex behavior already in simple epidemiological systems, the disease enhancement factor and the cross protection period [4].

Dengue fever is a major public health problem. With about half of the world's population at risk of acquiring a infection, disease severity is influenced by the immunological status of the individual, seronegative or seropositive, prior to a natural infection. While a primary dengue infection in humans is usually asymptomatic or results in mild disease clinical manifestation, the immunological response on exposure to a heterologous dengue serotype is complex, recognized to be a risk factor for progressing to severe disease characterized by hemorrhagic symptoms via the so-called Antibody-Dependent Enhancement (ADE) process [5–10].

Caused by four antigenically distinct virus, DENV-1, DENV-2, DENV-3 and DENV-4, the virus is transmitted by the infected Aedes mosquitoes. With approximately 400 million dengue infections every year [11–13], treatment

*Corresponding author
asrivastav@bcamath.org (A.K. Srivastav); vsteindorf@bcamath.org (V. Steindorf); nstollenwerk@bcamath.org (N. Stollenwerk); maguiar@bcamath.org (M. Aguiar)
ORCID(s): 0000-0003-3786-9159 (A.K. Srivastav); 0000-0002-0707-9511 (V. Steindorf)

of uncomplicated dengue cases is only supportive, while severe dengue cases require careful attention and proactive treatment of eventual hemorrhagic symptoms.

The World Health Organization (WHO) advocates combined control approaches for dengue control, and a safe, effective and affordable dengue vaccine against the four serotypes (tetravalent vaccine) would represent a significant advance for the control of the disease. Up to date, two tetravalent dengue vaccines have completed the phase 3 clinical trial: Dengvaxia, developed by Sanofi Pasteur that is now licensed in several countries [14], and the Qdenga (TAK-003) vaccine, developed by Takeda Pharmaceutical Company [15, 16]. While Dengvaxia has resulted in serious adverse events in seronegative individuals compared with age-matched seronegative controls [17–22], long-term surveillance consisting of prudent and careful observation of Qdenga vaccine recipients is required [23, 24], since serotype specific negative vaccine efficacy was observed for vaccinated seronegative individuals [25].

Mathematical models describing dengue fever epidemiology go back to 1970 [26]. To date, various aspects of the disease have been studied through mathematical models. A careful review of dengue modeling framework was recently published [27], where three structural multi-strain approaches were studied, the within-host, the vector-host, and the host-to-host transmission models. The within-host framework is built to describe viral replication and immunological responses affecting differently disease outcomes in primary and secondary infections, see e.g. [28, 29], while the other two approaches aim to describe disease transmission at population level. On the one hand, the host-to-host approach describes the disease transmission dynamics considering a simplified host-host contact and including the effect of seasonality to mimic abundance of mosquito population, see e.g. [4, 17, 30–38], on the other hand, the vector-host approach considers the explicit dynamics for the mosquito population affecting the disease transmission dynamics, see e.g. [34, 39, 40].

Coupling vector dynamics into the host-host modeling framework is critical to evaluate the impact of disease control at population level, since vector control to reduce mosquito population is the mostly used public health intervention measure worldwide. Vector-host dengue models dealing with optimal control problems are often proposed to evaluate the effect of a different combination of intervention measures, from disease transmission awareness and vaccination, including the novel strategy of transgenic vectors carrying the bacteria Wolbachia to mosquito population, see e.g. references [41–45]. These models have provided valuable information on the effect of such control measures at the population level. However, their formulation are often simplified such that important biological features are often not well integrated.

Aiming at evaluating the impact of the available public health measures to control the spreading of dengue fever, we propose a modeling framework that couples explicitly the vector dynamic into the two-serotype host model [46] that is needed to capture differences between primary and secondary infections. The optimal control problem is proposed to evaluate the effect of three different control measures on disease prevalence: i) self-protection measures against mosquito bites, ii) vector control programs to reduce mosquito population and iii) vaccination of seropositive individuals only, following the recent recommendation by the WHO [47].

This paper is organized as follows. The mathematical model is described in Section 2, where we discuss the boundedness of solutions and present the model analysis. In Section 3, a detailed sensitivity analysis is conducted to identify the model key parameters. The optimal control model is described in Section 4 with the results presented for different scenarios of disease control in Section 5. The paper is finalized with discussion and conclusion remarks.

2. The two-infection vector-host dengue model

The proposed two-infection vector-host dengue model is a refined version of the model previously proposed by Rashkov and Kooi, see reference [40], where the explicit mosquito population dynamics is coupled to the host transmission model proposed by [4, 48]. Although the incorporation of vector dynamics in a simple SIR model is straightforward, the multi-strain aspect increases the complexity of the system.

For the host modeling framework, we use an SIR-SIR type model [46]. The model is extended to include strain structure of pathogens. For the sake of simplicity, only two different dengue serotypes $i = 1, 2$ are considered, and therefore, only two infections are possible. This constraint is justified in [4, 30], showing that this minimalistic framework is complex enough to describe differences between primary and secondary infections, with a qualitatively good agreement between model simulation and empirical data.

For the host dynamics, susceptible individuals are stratified by their immunological status prior to a natural infection, seronegative S, i.e. susceptible individuals who were never exposed to any dengue serotype, and seropositive S_i, with $i = 1, 2$ i.e. susceptible individuals who were already exposed to one of the dengue serotypes. Hence,

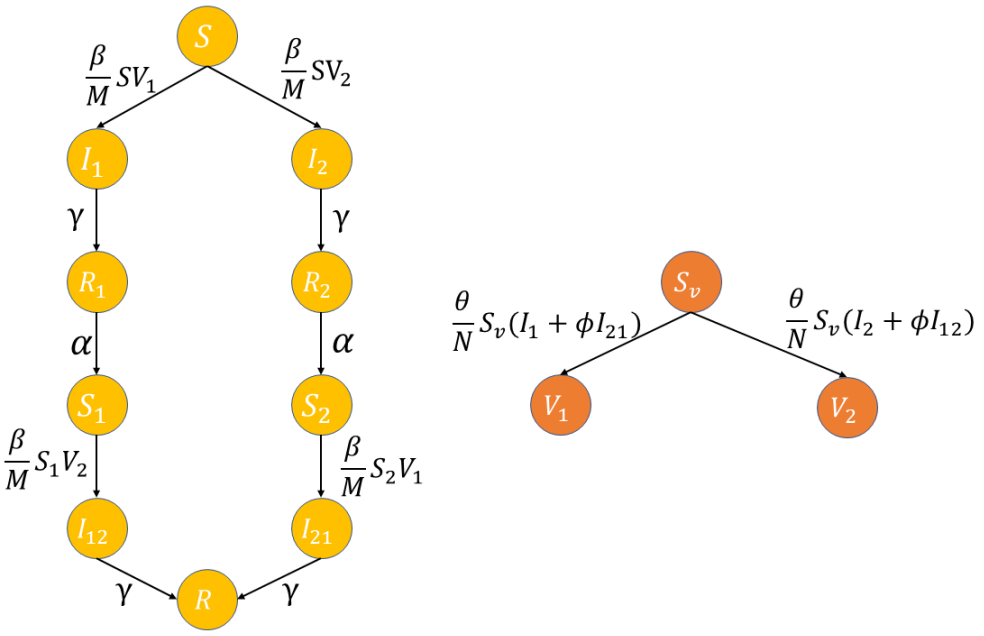

Figure 1: Flow chart of the host model in yellow, and the vector model in orange. Circles represent the compartments for each disease-related stage (for humans) and infection-related stage (for mosquitoes) with arrows indicating the transitions to coupling the systems.

the disease related states in humans are: primarily infected individuals with strain type 1, I_1, or strain type 2, I_2, recovered from the first infection with strain 1, R_1, or strain 2, R_2, seropositive infected individuals experiencing a secondary infection with strain type 2, I_{12}, previously infected with serotype 1 (S_1), and seropositive infected individuals experiencing a secondary infection with strain type 1, I_{21}, previously infected with serotype 1 (S_2). Finally, recovered and life-long immune individuals R. The demographic rate μ is included, with natural mortality and birth rates assumed to be equal, hence assuming a constant population size N for humans.

For the vector dynamics, we use the SI type model, an extension of the proposed model in references [17, 39], since mosquitoes remain infected with a unique strain type throughout their entire life spam. The system is coupled with the host model as such: susceptible mosquitoes S_v become infected with strain type 1, V_1, or with strain type 2, V_2, after biting an infected host with serotype 1 or 2 respectively. The demographic rate ν is included, with natural mortality and birth rates assumed to be equal, hence assuming a constant population size M for mosquitoes.

Human infection occurs when an infected mosquito V_i, with $i = 1, 2$, with bites a susceptible seronegative or seropositive human S, S_i. Differently from the mosquitoes, humans hosts can acquire up to two infections since birth, each infection with a single strain at time, due to the life long immunity conferred after an infection. Note that a secondary infection can only occur with a distinct (heterologous) serotype than the one causing a primary infection, and has higher risk of severe disease manifestation in humans via the ADE process (parametrized by the scaling by the disease enhancement factor ϕ). While the value of ϕ differentiates the secondary infection transmission rate from the baseline infectivity of primary infection θ, it can be tuned to reflect different situations: a value of $\phi > 1$ reflects the fact that severe cases, i.e. secondary infections, have larger infectivity than mild cases, i.e. primary infections due to, for example, the enhanced viral load from the the ADE process, while $\phi < 1$ indicates that severe cases contribute less to the force of infection than primary infections, due to, for example, their lower interaction with mosquitoes once they are hospitalized and isolated [4, 30–33, 48, 49]. Conversely, susceptible mosquitoes (S_v) become infected at rate θ after biting infected individuals in a primary infection or at rate $\phi\theta$ after biting infected individuals experiencing a secondary infection. Infected mosquito transmit the virus to a susceptible host with the transmission rate β.

The model dynamics illustrated in Fig. 1 is a refinement of the model proposed in [40]. The main differences are highlighted in blue in the corresponding coupled ODE system (1), for the following considerations: i) reduction in transmissibility from humans to vectors when vectors acquire the infection from humans experiencing their secondary

infection ($\phi < 1$), as proposed in [48], and ii) symmetric transmission rate from an infected mosquito to seronegative and seropositive susceptible humans (β).

$$
\begin{aligned}
\dot{S} &= -\frac{\beta}{M} S(V_1 + V_2) + \mu(N - S), \\
\dot{I}_1 &= \frac{\beta}{M} S V_1 - (\gamma + \mu) I_1, \\
\dot{I}_2 &= \frac{\beta}{M} S V_2 - (\gamma + \mu) I_2, \\
\dot{R}_1 &= \gamma I_1 - (\alpha + \mu) R_1, \\
\dot{R}_2 &= \gamma I_2 - (\alpha + \mu) R_2, \\
\dot{S}_1 &= \alpha R_1 - \mu S_1 - \frac{\beta}{M} S_1 V_2, \\
\dot{S}_2 &= \alpha R_2 - \mu S_2 - \frac{\beta}{M} S_2 V_1, \\
\dot{I_{12}} &= \frac{\beta}{M} S_1 V_2 - (\gamma + \mu) I_{12}, \\
\dot{I_{21}} &= \frac{\beta}{M} S_2 V_1 - (\gamma + \mu) I_{21}, \\
\dot{R} &= \gamma(I_{12} + I_{21}) - \mu R, \\
\dot{S}_v &= -\frac{\theta}{N} S_v(I_1 + I_2 + \phi(I_{21} + I_{12})) + \nu(M - S_v), \\
\dot{V}_1 &= \frac{\theta}{N} S_v(I_1 + \phi I_{21}) - \nu V_1, \\
\dot{V}_2 &= \frac{\theta}{N} S_v(I_2 + \phi I_{12}) - \nu V_2.
\end{aligned}
\tag{1}
$$

Both dengue serotypes are assumed to be symmetric, see references [35, 50], and therefore the dynamics of the complete vector-host model is described as follows. Susceptible individuals become infected with rate β after a mosquito bite, recovering with a recovery rate γ. Although human hosts remain lifelong immune against the strain causing a primary infection, a short Temporary Cross-Immunity (TCI) period α, conferred by the antibody levels produced during the immune response of the first infection [28, 29], is included, protecting these individuals against an immediate secondary dengue infection. Waning protection occurs with individuals becoming susceptible seropositive after the TCI period, able to acquire a secondary infection with a heterologous dengue serotype. The clinical response on exposure to a second serotype is complex due to the ADE process, where the pre-existing antibodies to previous dengue infection do not neutralize but rather enhance the new infection. Individuals experiencing a secondary infection are assumed to develop severe disease prone to hospitalization, assumed to have a slightly lower transmission rate ($\phi < 1$) than individuals experiencing a primary infection, according to the results published in reference [51], where persons with unapparent dengue infections were more infectious to mosquitoes than clinically symptomatic patients.

2.1. Positivity and boundedness of the solutions

In this section, the positivity and boundedness of the solutions of the system (1) is proved. From the system (1), the following is verified

$$
\left.\frac{dS}{dt}\right|_{S=0} = \mu N > 0, \quad \left.\frac{dI_1}{dt}\right|_{I_1=0} = \frac{\beta}{M} S V_1 \geq 0, \quad \left.\frac{dI_2}{dt}\right|_{I_2=0} = \frac{\beta}{M} S V_2 \geq 0, \quad \left.\frac{dR_1}{dt}\right|_{R_1=0} = \gamma I_1 \geq 0, \quad \left.\frac{dR_2}{dt}\right|_{R_2=0} = \gamma I_2 \geq 0,
$$

$$
\left.\frac{dS_1}{dt}\right|_{S_1=0} = \alpha R_1 > 0, \quad \left.\frac{dS_2}{dt}\right|_{S_2=0} = \alpha R_2 \geq 0, \quad \left.\frac{dI_{12}}{dt}\right|_{I_{12}=0} = \frac{\beta}{M} S_1 V_2 \geq 0, \quad \left.\frac{dI_{21}}{dt}\right|_{I_{21}=0} = \frac{\beta}{M} S_2 V_1 \geq 0,
$$

$$
\left.\frac{dR}{dt}\right|_{R=0} = \gamma(I_{12}+I_{21}) \geq 0, \quad \left.\frac{dS_v}{dt}\right|_{S_v=0} = \nu > 0, \quad \left.\frac{dV_1}{dt}\right|_{V_1=0} = \frac{\theta}{N} S_v(I_2+\phi I_{21}) \geq 0 \quad \left.\frac{dV_2}{dt}\right|_{V_2=0} = \frac{\theta}{N} S_v(I_1+\phi I_{12}) \geq 0.
$$

All the above inequalities are non-negative on the boundary planes. Hence, if we begin in the interior of the non-negative bounded cone R_+^{10}, we will remain in this cone, since the vector field direction is not outward of the bounding planes. Thus, the solutions of the system (1) being non-negative is guaranteed. Furthermore, it is possible to conclude that the total populations N and M satisfies

$$\frac{dN}{dt} = 0$$

and

$$\frac{dM}{dt} = 0.$$

Therefore, the total human population $N = S + I_1 + I_2 + S_1 + S_2 + R_1 + R_2 + I_{12} + I_{21} + R$ and the total mosquito population $M = S_v + V_1 + V_2$ are constant, and all the solutions $S, I_1, I_2, S_1, S_2, R_1, R_2, I_{12}, I_{21}, R$ are bounded by N. Similarly, the solutions S_v, V_1, V_2 are bounded by M. Hence, the biologically feasible region of the model system (1) is given by the following positive invariant set:

$$\begin{aligned}\Omega = \{&(S, I_1, I_2, S_1, S_2, R_1, R_2, I_{12}, I_{21}, V_1, V_2) \in R^{11} \mid 0 \le S, I_1, I_2, S_1, S_2, R_1, R_2, I_{12}, I_{21} \le N, \\ &S + I_1 + I_2 + S_1 + S_2 + R_1 + R_2 + I_{12} + I_{21} \le N,\ 0 \le S_v, V_1, V_2 \le M, \text{and} S_v + V_1 + V_2 \le M\}.\end{aligned} \tag{2}$$

All parameters are non-negative constants and thus, in order to work with the fraction of each sub-population we define

$$\begin{gathered} s = \frac{S}{N}, i_1 = \frac{I_1}{N}, i_2 = \frac{I_2}{N}, r_1 = \frac{R_1}{N}, r_2 = \frac{R_2}{N} \\ s_1 = \frac{S_1}{N}, s_2 = \frac{S_2}{N}, i_{12} = \frac{I_{12}}{N}, i_{21} = \frac{I_{21}}{N}, r = \frac{R}{N} = r, \\ s_v = \frac{S_v}{M}, v_1 = \frac{V_1}{M}, v_2 = \frac{V_2}{M}. \end{gathered}$$

The system (1) can be rewritten in the following form

$$\begin{aligned}
\dot{s} &= -\beta s(v_1 + v_2) + \mu(1 - s), \\
\dot{i_1} &= \beta s v_1 - (\gamma + \mu) i_1, \\
\dot{i_2} &= \beta s v_2 - (\gamma + \mu) i_2, \\
\dot{r_1} &= \gamma i_1 - (\alpha + \mu) r_1, \\
\dot{r_2} &= \gamma i_2 - (\alpha + \mu) r_2, \\
\dot{s_1} &= \alpha r_1 - \mu s_1 - \beta s_1 v_2, \\
\dot{s_2} &= \alpha r_2 - \mu s_2 - \beta s_2 v_1, \\
\dot{i_{12}} &= \beta s_1 v_2 - (\gamma + \mu) i_{12}, \\
\dot{i_{21}} &= \beta s_2 v_1 - (\gamma + \mu) i_{21}, \\
\dot{r} &= \gamma(i_{12} + i_{21}) - \mu r, \\
\dot{s_v} &= -\theta s_v(i_1 + \phi i_{21} + i_2 + \phi i_{12}) + \nu(1 - s_v), \\
\dot{v_1} &= \theta s_v(i_1 + \phi i_{21}) - \nu v_1, \\
\dot{v_2} &= \theta s_v(i_2 + \phi i_{12}) - \nu v_2.
\end{aligned} \tag{3}$$

where the solution of each equation describes the fraction of the prevalence of each sub-population (class).

2.2. Model analysis

2.2.1. Disease-free equilibrium E_0

The Equation System (3) has the disease-free equilibrium, given by

$$E_0 = (1, 0, 0, 0, 0, 0, 0, 0, 0, 0, 1, 0, 0)\,.$$

2.2.2. *The basic reproduction number* $\mathcal{R}_0$

The basic reproduction number of the Equation System (3) is given by

$$\mathcal{R}_0 = \sqrt{\frac{\theta\beta}{\nu(\gamma+\mu)}}.$$

The term $\frac{\beta}{(\gamma+\mu)}$ denotes the expected number of infected mosquitoes generated by a single infected human during his infectious period. Similarly, the term $\frac{\theta}{\nu}$ denotes the expected number of infected humans generated by a single infected mosquito during his infectious period. The product of these two terms, $\mathcal{R}_0$, represents the number of infected hosts generated by a single infected human and a single infected mosquito during the whole infectious period. Calculations of the $\mathcal{R}_0$ and details are given in the Appendix (6).

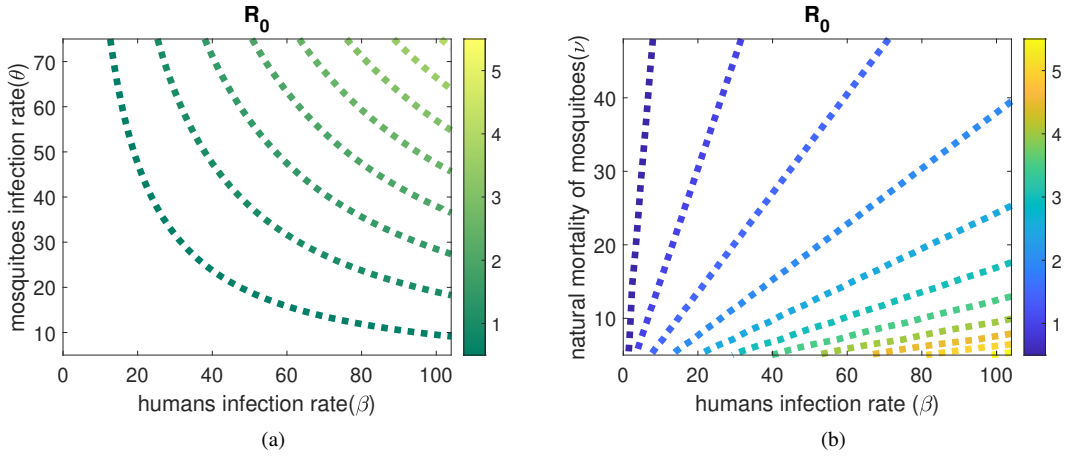

Figure 2: Effect of the transmission rates on $\mathcal{R}_0$ values. In (a) we vary the human transmission rate β and the mosquito transmission θ. In (b) the human transmission rate and natural mortality rate for mosquitoes ν are varied. The baseline values of the model parameters are shown in Table 1.

Figure 2(a) illustrates the impact of the infection rates of humans and mosquitoes on the basic reproduction number $\mathcal{R}_0$, while as in Fig. 2(b) the natural mortality rate of mosquitoes is shown. The choice of these parameters are in accordance with the sensitivity analysis performed in Section 3, and are reflecting on the optimal control problem formulated in Section 4. Both, the human transmission rate (β) and the mosquito transmission rate (θ) have a direct effect on the basic reproduction number $\mathcal{R}_0$, that is, if the values for β and θ increase (or decrease), then the value of $\mathcal{R}_0$ will increase (or decrease) as well. As a result, disease spreading could be reduced by using public health measures able to reduce the viral transmission from humans to vectors and from vectors to humans, such as, for example, the use of repellents, mosquito nets and effective vaccines. On the other hand, Figure 2(b) shows an indirect effect of the mortality rates of mosquitoes (ν), that is, if mosquito mortality increases, the value of $\mathcal{R}_0$ decreases. Here, the disease spreading could be also controlled by efficacious mosquito eradication programs.

3. Sensitivity analysis (PRCC)

Aiming to identify and rank the key parameters whose uncertainties contribute more to the variability of the disease prevalence (the model output), we use the approach described in references [52, 53], and perform a global sensitivity analysis of system. The sensitivity analysis of the vector-host system is performed using two statistical techniques, the Latin Hypercube Sampling (LHS) and Partial Rank Correlation Coefficients (PRCCs).

The LHS method varies all the parameters together in a defined interval and in a systematic way, generating and providing a quasi-random sample of the parameter values, the so called LHS matrix, that will be used for the PRCC plot. The PRCC method measures the monotonicity between the LHS parameters and the model output after removing

the linear effects of all parameters, except the parameter of interest. Hence, it connects the input parameters and the response function by assigning values between -1 and 1. These values represent the strength of correlation between them, while the sign represents the type of correlations, positive or negative.

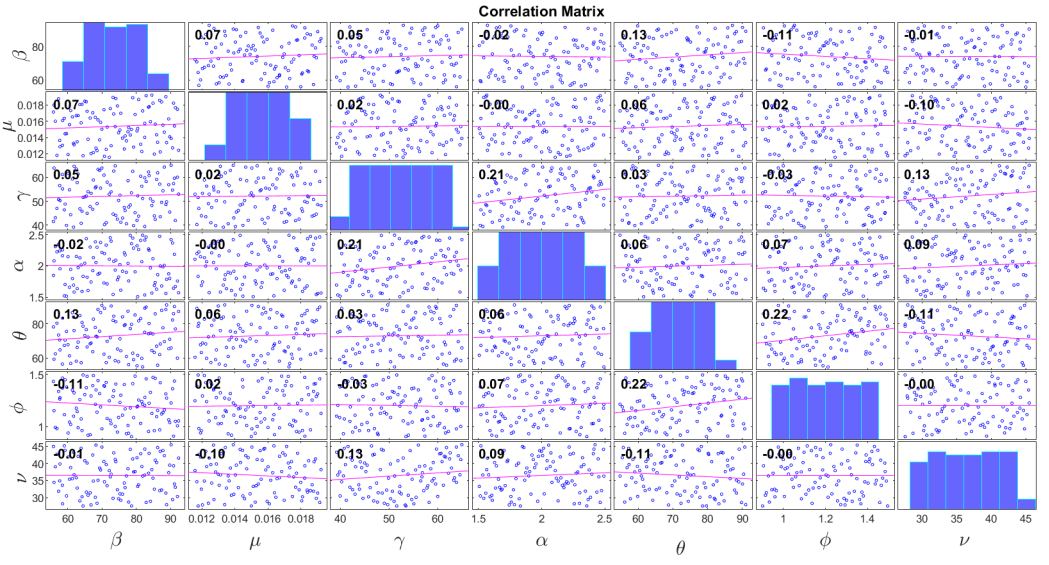

Figure 3: LHS Matrix correlation for the model parameters. With 200 iterations per parameter, we consider $\pm 25\%$ deviation from the baseline parameter value listed in Table 1.

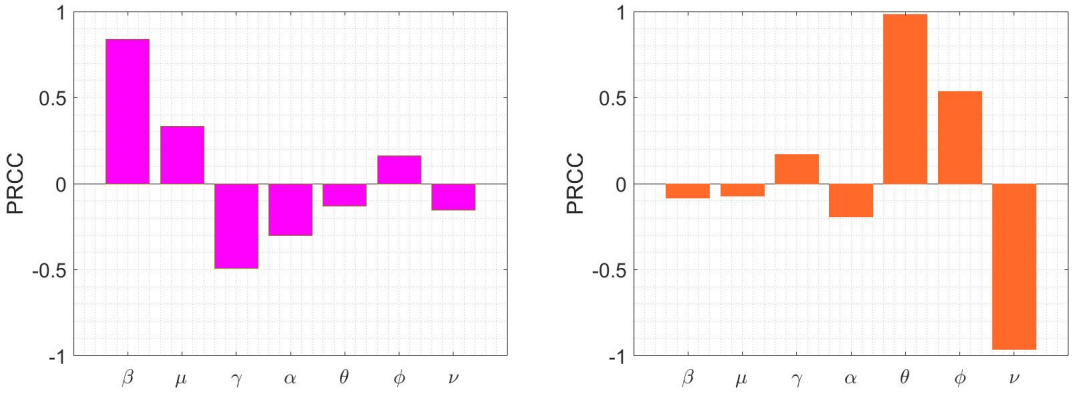

(a) Output infected host population $i = i_1 + i_2 + i_{12} + i_{21}$

(b) Output infected mosquito population $v = v_1 + v_2$

Figure 4: Effect of model parameters uncertainties. In (a) PRCC for the infected human population and in (b) PRCC for the infected mosquito population. The baseline parameter values used in these computations are listed in Table 1.

In detail, for the LHS method, we consider an uniform distribution for each input parameter. With $\pm 25\%$ deviation from the baseline parameter values (see Table 1), 200 simulations are obtained. Results are shown in Figure 3, where the correlation between each parameter and the p-values are shown. Strong correlation is characterized by p-values below 0.05. For the PRCC analysis, the epidemiological parameters $\beta, \gamma, \alpha, \mu, \phi, \theta$ and ν, are considered as input parameters, while the infected host variables $i = (i_1+i_2+i_{12}+i_{21})$ and the infected mosquitoes variables $v = v_1+v_2$, are considered as response functions, with nonlinear and monotone relationships being recognized between the infected populations

Table 1
The vector-host model baseline parameters obtained from references [4, 40, 46, 48, 54]. Other parameter values eventually used for numerical simulations will be explicitly stated in the specific figure captions.

parameters		description	baseline values
β	:	transmission rate from vector to humans	$104y^{-1}$ (2 γ)
γ	:	recovery rate	$52y^{-1}$ (7 days)
α	:	temporary cross-immunity rate	$2y^{-1}$ (6 months)
ϕ	:	ratio of secondary infections contribution to the overall force of infection	0.6 or 2.6
μ	:	natural mortality and birth rates (humans)	$1/65y^{-1}$
θ	:	transmission rate from host to vector	$73y^{-1}$ (2 ν)
ν	:	natural mortality and birth rate (mosquito)	$36.5y^{-1}$ (20 days)
ρ	:	vaccine distribution to seropositive per time unit	0.2
η	:	additional mosquito killing rate	0.4
population variables			
N	:	total human population	1000
M	:	total mosquito population	10000
control variables			
$u_1(t)$	:	measures against mosquito bites	(0, 1)
$u_2(t)$	:	measures to reduce mosquito population	(0, 1)
$u_3(t)$	:	vaccination of seropositive individuals	(0, 1)
weight constants			
$A_1 = A_2 = A_3 = A_4$	:	weight constant for infective human population	1
A_5	:	weight constant for mosquito population	0
D_1	:	weight constant for control u_1	0.3
D_2	:	weight constant for control u_2	0.9
D_3	:	weight constant for control u_3	0.7

and the input parameters, see Figure 4. In Fig. 4(a), the correlations for the total infected human population are shown, in which the parameters β, μ and ϕ have a direct correlation with the disease spreading, i.e, the increase/decrease of these parameters values lead to increase/decrease of infections. On the other hand, the parameter γ has a indirect correlation effect with the total infected human population, i.e, the increase of γ value will decrease the number of infections. Similarly, the positive correlations for the infected mosquito population are observed for the following parameters θ and ϕ, while the parameter ν has a negative correlation effect, see Fig. 4(b).

These results will be used to evaluate the impact of the available public health measures for dengue control targeting the parameters with highest impact on the model output.

4. The two-infection vector-host dengue model with optimal control

The results presented in the previous Section have shown that the transmission rates for human hosts and vectors, β and θ, the disease enhancement factor ϕ and the mosquitoes mortality rate ν are the model parameters affecting most the dynamics of the system, with high impact on disease prevalence. Our model described in Equation System (3) is extended to include the available control measures associated with each one of the parameters and will be analysed as an optimal control problem. The control methods are divided into three categories.

i. **Control measures to reduce disease transmission $u_1(t)$:**
In the absence of a save and effective vaccine, self-protection measures such as the use of repellent or bed nets, for example, are effective strategies against mosquito bites reducing transmission from mosquito to humans (β) and from humans to mosquitoes (θ).
The term $u_1(t)$ is incorporated into the system to represent the reduction in transmissibility from humans to vectors and from vectors to humans.

ii. **Control measures to reduce mosquito population $u_2(t)$:**
Vector control includes mosquito surveillance combined with different methods to reduce mosquito population at larger geographical scales. The existing mosquito control programs aim at eliminating mosquito larval habitats, applying larvicides to kill mosquito larvae, or spraying insecticides from trucks or aircrafts to kill adult mosquitoes [55].
The term $u_2(t)$ is incorporated into the system to represent the reduction of mosquito populations by using insecticide treatment applied to large areas, and hence, more costly than the self protection measures against mosquito bites. Moreover, as the insecticide product may vary in quality and effectiveness, we incorporate the term as η as an additional killing rate for mosquitoes as proposed by [56].

iii. **Vaccine administration to seropositive individuals $u_3(t)$:**
The sustained failures to control vector abundance using classical vector control methods have resulted in a large effort to develop new vaccines. A safe, effective and affordable dengue vaccine against the four serotypes (tetravalent vaccine) would represent a significant advance for the control of the disease [13]. Up to date, two tetravalent dengue vaccines have completed their phase 3 clinical trial, the Dengvaxia vaccine [14, 57, 58], developed by Sanofi Pasteur, and the Qdenga (TAK-003) vaccine, developed by Takeda Pharmaceutical Company [25, 59, 60]. The Dengvaxia vaccine was licensed in 2016 and used in mass vaccination programs in the Philippines and in Brazil in spite of vaccine trial results showing serious adverse events in vaccinated children without history of previous dengue infection (seronegative) [17, 61]. The risks behind the Dengvaxia vaccine recommendation was exhaustively discussed [17, 19–21, 62–64], after an age-structured model [62], validated and parametrized with the available vaccine trial data [14, 57, 58], has shown that a significant reduction of hospitalizations would be only possible when this vaccine would be given to individuals with a history of previous dengue infection (seropositive). These results contradicted the results from the WHO-SAGE modeling group [65] and by the Sanofi Pasteur's modelling group [66], predicting a significant increase of hospitalizations when this vaccine would be administered without prior population screening, i.e. vaccinating both seropositive and seronegative individuals [20, 21, 62]. The individuals' serostatus prior to vaccination was the determinant for this vaccine efficacy and its possible benefits [21]. We note that eventually these results have led the vaccine manufacturer to perform new tests [67], changing this vaccine recommendation by the World Health Organization (WHO) in April 2018 [47]. With that said, it is important to mention that to a realistic evaluation of the effect of this vaccine in a ethical vaccination programme [63] would be only possible by vaccinating seropositive individuals only. Although this specific recommendation would involve population screening prior to vaccination, the initial assumption was to consider that measure to be slightly less costly that the vector control programs that are used widely and more often that the first.
Here, differently from the already existing optimal control modeling approaches, we consider vaccinating only seropositive individuals, with the cost of population screening prior to vaccination included into the cost of vaccine administration. Hence, to evaluate the impact of this vaccination strategy on the overall number of infections, while keeping the costs at its minimum value, vaccination of seropositive individuals S_1, and S_2 is included into the system as $\rho u_3(t)$ term, following the current vaccine recommendation strategy. The parameter ρ refers to the number of vaccine doses distributed to seropositive individuals per time unit.

The extended ODE system with controls is shown in Equation System (4):

$$
\begin{aligned}
\dot{s} &= -(1-u_1)\beta s(v_1+v_2)+\mu(1-s),\\
\dot{i_1} &= (1-u_1)\beta s v_1-(\gamma+\mu)i_1,\\
\dot{i_2} &= (1-u_1)\beta s v_2-(\gamma+\mu)i_2,\\
\dot{r_1} &= \gamma i_1-(\alpha+\mu)r_1,\\
\dot{r_2} &= \gamma i_2-(\alpha+\mu)r_2,\\
\dot{s_1} &= \alpha r_1-\mu s_1-(1-u_1)\beta s_1 v_2-\rho u_3 s_1,\\
\dot{s_2} &= \alpha r_2-\mu s_2-(1-u_1)\beta s_2 v_1-\rho u_3 s_2,\\
\dot{i_{12}} &= (1-u_1)\beta s_1 v_2-(\gamma+\mu)i_{12},\\
\dot{i_{21}} &= (1-u_1)\beta s_2 v_1-(\gamma+\mu)i_{21},\\
\dot{r} &= \rho u_3 s_1+\rho u_3 s_2+\gamma(i_{12}+i_{21})-\mu r,\\
\dot{s_v} &= -(1-u_1)\theta s_v(i_1+\phi i_{21}+i_2+\phi i_{12})+(\nu+\eta u_2)(1-s_v),\\
\dot{v_1} &= (1-u_1)\theta s_v(i_1+\phi i_{21})-(\nu+\eta u_2)v_1,\\
\dot{v_2} &= (1-u_1)\theta s_v(i_2+\phi i_{12})-(\nu+\eta u_2)v_2.
\end{aligned}
\tag{4}
$$

4.1. The optimal control problem formulation

While the WHO advocates a combined control approaches for vector-borne diseases, the core idea of this work is to explore the impact of different strategies to asses its effects on disease prevalence.

Using the optimal control theory, we analyze the behavior of the model shown in Equation System (4). The cost functional corresponding to the total cost incurred for the control measures for a fixed time t_f, which need to be minimized, is given by:

$$
J=\int_0^{t_f}(A_1 i_1+A_2 i_2+A_3 i_{12}+A_4 i_{21}+A_5(s_v+v_1+v_2)+\frac{1}{2}D_1 {u_1}^2+\frac{1}{2}D_2 {u_2}^2+\frac{1}{2}D_3 {u_3}^2)dt. \tag{5}
$$

Here the parameters $A_1 \geq 0$, $A_2 \geq 0$, $A_3 \geq 0$, $A_4 \geq 0$ represent the constant cost for minimizing disease prevalence in humans while the parameter $A_5 \geq 0$ represents the constant cost for minimizing mosquito population. The parameters $D_1 \geq 0$ and $D_2 \geq 0$ are the cost of the control strategies used to reduce mosquito bites and mosquito population respectivelly while the parameter $D_3 \geq 0$ is the cost for vaccinating seropositive individuals.

Our objective is to find the control ${u_1}^*$, ${u_2}^*$ and ${u_3}^*$, such that

$$
J({u_1}^*,{u_2}^*,{u_3}^*)=\min_{u_1,u_2,u_3\in\mathbb{Q}} J(u_1,u_2,u_3),
$$

where $\mathbb{Q}$ is the control set which is defined as $\mathbb{Q}=\{u_1,u_2,u_3 : \text{measurable and } 0\leq u_1,u_2,u_3\leq 1\}$ and $t\in[0,t_f]$.

4.2. Existence and characterization of optimal controls

Here we establish the existence of control functions that minimize the cost functional J. The Lagrangian of this problem is defined as:

$$
L(i_1,i_2,i_{12},i_{21},s_v,v_1,v_2,u_1,u_2,u_3)=A_1 i_1+A_2 i_2+A_3 i_{12}+A_4 i_{21}+A_5(s_v+v_1+v_2)+\frac{1}{2}D_1 {u_1}^2+\frac{1}{2}D_2 {u_2}^2+\frac{1}{2}D_3 {u_3}^2.
$$

Theorem 1. *There exist optimal controls ${u_1}^*,{u_2}^*,{u_3}^*\in\mathbb{Q}$ such that*

$$
J({u_1}^*,{u_2}^*,{u_3}^*)=\min J({u_1}^*,{u_2}^*,{u_3}^*)
$$

subject to system (4).

PROOF. To establish this result, we follow the Theorem 3.1 proved in [68] for the existence of optimal controls. As discussed above, the state variables are bound to the control set $\mathbb{Q}$. Furthermore, Lipschitz condition with respect to state variables is satisfied by the right hand part of the equation system (4). The control set $\mathbb{Q}$ is also convex and closed by the convexity definition, and the system (4) is linear in terms of the control variables. The integrand of the functional

$$L = A_1 i_1 + A_2 i_2 + A_3 i_{12} + A_4 i_{21} + A_5(s_v + v_1 + v_2) + \frac{1}{2} D_1 {u_1}^2 + \frac{1}{2} D_2 {u_2}^2 + \frac{1}{2} D_3 {u_3}^2$$

is convex on the control set $\mathbb{Q}$ due to the quadratic nature of the control variables. Moreover,

$$L = A_1 i_1 + A_2 i_2 + A_3 i_{12} + A_4 i_{21} + A_5(s_v + v_1 + v_2) + \frac{1}{2} D_1 {u_1}^2 + \frac{1}{2} D_2 {u_2}^2 + \frac{1}{2} D_3 {u_3}^2 \geq \frac{1}{2} D_1 {u_1}^2 + \frac{1}{2} D_2 {u_2}^2 + \frac{1}{2} D_3 {u_3}^2.$$

Considering $c_1 = min(A_1, A_2, A_3, A_4, D_1, D_2, D_3) > 0$ and $g(u_1, u_2, u_3) = c_1(\frac{1}{2} D_1 {u_1}^2 + \frac{1}{2} D_2 {u_2}^2 + \frac{1}{2} D_3 {u_3}^2)$, $L \geq g(u_1, u_2, u_3)$ holds true and g is continuous, satisfying the condition $\mid (u_1, u_2, u_3) \mid^{-1} g(u_1, u_2, u_3) \to \infty$ whenever $\mid (u_1, u_2, u_3) \mid \to \infty$. Thus, all the conditions for the existence of controls are fulfilled (for more details, please see [68, 69] and references therein. Hence, the result is proved. □

The existing optimal solution for our problem can be found with Pontryagin's Minimum principle [69] as follows. We define the Hamiltonian $\mathcal{H}$ by

$$\mathcal{H} = L(i_1, i_2, i_{12}, i_{21}, s_v, v_1, v_2, u_1, u_2, u_3) + \sum_{i=1}^{13} \lambda_i \frac{d f_i}{dt}, \tag{6}$$

where λ_i, $i = 1 \ldots 13$ are the adjoint variables (the time-varying Lagrange multipliers).

The conditions for optimizing the Hamiltonian are described in the following theorems.

Theorem 2. *Let u_i^*, $1 \leq i \leq 3$, be the optimal control functions and $s^*, i_1^*, i_2^*, r_1^*, r_2^*, s_1^*, s_2^*, i_{12}^*, i_{21}^*, r^*, s_v^*, v_1^*, v_2^*$, the corresponding state variables of the optimal control problem (1)-(2). Then there exists adjoint variables $\lambda = (\lambda_1, \lambda_2, \ldots, \lambda_{13})^T \in \mathbb{R}^{13}$, which satisfies the following equations*

$$\begin{aligned}
\frac{d\lambda_1}{dt} &= -\frac{\partial H}{\partial s} &&= (1-u_1)\beta v_1(\lambda_1 - \lambda_2) + (1-u_1)\beta v_2(\lambda_1 - \lambda_3) + \lambda_1 \mu \\
\frac{d\lambda_2}{dt} &= -\frac{\partial H}{\partial i_1} &&= -A_1 + \lambda_2(\gamma + \mu) + (1-u_1)\theta s_v(\lambda_{11} - \lambda_{12}) \\
\frac{d\lambda_3}{dt} &= -\frac{\partial H}{\partial i_2} &&= -A_2 + \lambda_3(\gamma + \mu) + (1-u_1)\theta s_v(\lambda_{11} - \lambda_{13}) \\
\frac{d\lambda_4}{dt} &= -\frac{\partial H}{\partial r_1} &&= (\alpha + \mu)\lambda_4 - \alpha\lambda_6 \\
\frac{d\lambda_5}{dt} &= -\frac{\partial H}{\partial r_2} &&= (\alpha + \mu)\lambda_5 - \alpha\lambda_7 \\
\frac{d\lambda_6}{dt} &= -\frac{\partial H}{\partial s_1} &&= \mu\lambda_6 + \rho u_3(\lambda_6 - \lambda_{10}) + (1-u_1)\beta v_2(\lambda_6 - \lambda_8) \\
\frac{d\lambda_7}{dt} &= -\frac{\partial H}{\partial s_2} &&= \mu\lambda_7 + \rho u_3(\lambda_7 - \lambda_{10}) + (1-u_1)\beta v_1(\lambda_7 - \lambda_9) \\
\frac{d\lambda_8}{dt} &= -\frac{\partial H}{\partial i_{12}} &&= -A_3 + \lambda_8(\mu + \gamma) - \lambda_{10}\gamma + (1-u_1)\theta s_v \phi(\lambda_{11} - \lambda_{13}) \\
\frac{d\lambda_9}{dt} &= -\frac{\partial H}{\partial i_{21}} &&= -A_4 + \lambda_9(\mu + \gamma) - \lambda_{10}\gamma + (1-u_1)\theta s_v \phi(\lambda_{11} - \lambda_{12}) \\
\frac{d\lambda_{10}}{dt} &= -\frac{\partial H}{\partial r} &&= \lambda_{10}\mu \\
\frac{d\lambda_{11}}{dt} &= -\frac{\partial H}{\partial s_v} &&= -A_5 + (\nu + \eta u_2)\lambda_{11} + (1-u_1)\theta(i_1 + \phi i_{21})(\lambda_{11} - \lambda_{12}) + (1-u_1)\theta(i_2 + \phi i_{12})(\lambda_{11} - \lambda_{13})
\end{aligned}$$

$$\frac{d\lambda_{12}}{dt} = -\frac{\partial H}{\partial v_1} = -A_5 + (\nu + \eta u_2)\lambda_{12} + (1-u_1)\beta s(\lambda_1 - \lambda_2) + (1-u_1)\beta s_1\lambda_7$$
$$\frac{d\lambda_{13}}{dt} = -\frac{\partial H}{\partial v_2} = -A_5 + (\nu + \eta u_2)\lambda_{13} + (1-u_1)\beta s(\lambda_1 - \lambda_3) + (1-u_1)\beta s_1\lambda_6.$$

PROOF. Let $\widetilde{s}, \widetilde{i_1}, \widetilde{i_2}, \widetilde{r_1}, \widetilde{r_2}, \widetilde{s_1}, \widetilde{s_2}, \widetilde{i_{12}}, \widetilde{i_{21}}, \widetilde{r}, \widetilde{s_v}, \widetilde{v_1}, \widetilde{v_2}$ be the optimum values of $s, i_1, i_2, r_1, r_2, s_1, s_2, i_{12}, i_{21}, r, s_v, v_1, v_2$ respectively, and $\widetilde{\lambda_1}, \widetilde{\lambda_2}, \widetilde{\lambda_3}, \widetilde{\lambda_4}, \widetilde{\lambda_5}, \widetilde{\lambda_6}, \widetilde{\lambda_7}, \widetilde{\lambda_8}, \widetilde{\lambda_9}, \widetilde{\lambda_{10}}, \widetilde{\lambda_{11}}, \widetilde{\lambda_{12}}, \widetilde{\lambda_{13}}$ be the solution of the system of differential equations (4). By using [68, 69], we prove this theorem where the transversality conditions are given by

$$\lambda_i(t_f) = 0, \ i = 1 \dots 13. \tag{7}$$

Let $u_i^*, \ 1 \le i \le 3$, be the optimal control functions and $s^*, i_1^*, i_2^*, r_1^*, r_2^*, s_1^*, s_2^*, i_{12}^*, i_{21}^*, r^*, s_v^*, v_1^*, v_2^*$, the corresponding state variables. Then, the Pontryagin's Minimum Principle ensures the existence of the following adjoint variables $\lambda = (\lambda_1, \lambda_2, \dots, \lambda_{13})^T \in \mathbb{R}^{13}$, which satisfy the following canonical equations:

$$\frac{d\lambda_1}{dt} = -\frac{\partial H}{\partial s}, \ \frac{d\lambda_2}{dt} = -\frac{\partial H}{\partial i_1}, \ \frac{d\lambda_3}{dt} = -\frac{\partial H}{\partial i_2}, \ \frac{d\lambda_4}{dt} = -\frac{\partial H}{\partial r_1}, \ \frac{d\lambda_5}{dt} = -\frac{\partial H}{\partial r_2}, \ \frac{d\lambda_6}{dt} = -\frac{\partial H}{\partial s_1}, \ \frac{d\lambda_7}{dt} = -\frac{\partial H}{\partial s_2},$$
$$\frac{d\lambda_8}{dt} = -\frac{\partial H}{\partial i_{12}}, \ \frac{d\lambda_9}{dt} = -\frac{\partial H}{\partial i_{21}}, \ \frac{d\lambda_{10}}{dt} = -\frac{\partial H}{\partial r}, \ \frac{d\lambda_{11}}{dt} = -\frac{\partial H}{\partial s_v}, \ \frac{d\lambda_{12}}{dt} = -\frac{\partial H}{\partial v_1}, \ \frac{d\lambda_{13}}{dt} = -\frac{\partial H}{\partial v_2},$$

following the definition given in eq. (7), and where the H is the Hamiltonian defined in (6). Thus, the adjoint system can be obtained.

Theorem 3. *The optimal controls* $({u_1}^*, {u_2}^*, {u_3}^*)$ *which minimizes J over the region* Ω *are given by*

$${u_1}^* = min\{1, max(0, \widetilde{u_1})\}, {u_2}^* = min\{1, max(0, \widetilde{u_2})\}, {u_3}^* = min\{1, max(0, \widetilde{u_3})\},$$

where

$$\widetilde{u_1} = \frac{M_1}{D_1},$$

and

$$M_1 = \beta s v_1(\lambda_2 - \lambda_1) + \beta s v_2(\lambda_3 - \lambda_1) + \beta s_1 v_2(\lambda_8 - \lambda_6) + \beta s_2 v_1(\lambda_9 - \lambda_7) + \theta s_v(i_1 + \phi i_{21})(\lambda_{12} - \lambda_{11}) + \theta s_v(i_2 + \phi i_{12})(\lambda_{13} - \lambda_{11})$$

$$\widetilde{u_2} = \frac{\eta((1-s_v)\lambda_{11} + v_1\lambda_{12} + v_2\lambda_{13})}{D_2}$$

$$\widetilde{u_3} = \frac{(\rho s_1(\lambda_6 - \lambda_{10}) + \rho s_2(\lambda_7 - \lambda_{10}))}{D_3}.$$

PROOF. Using the optimality condition:

$$\frac{\partial \mathcal{H}}{\partial u_1} = 0, \ \frac{\partial \mathcal{H}}{\partial u_2} = 0, \ \frac{\partial \mathcal{H}}{\partial u_3} = 0.$$

we get,

$$\frac{\partial \mathcal{H}}{\partial u_1} = D_1 u_1 + \beta s v_1(\lambda_1 - \lambda_2) + \beta s v_2(\lambda_1 - \lambda_3) + \beta s_1 v_2(\lambda_6 - \lambda_8) + \beta s_2 v_1(\lambda_7 - \lambda_9) + \theta s_v(i_1 + \phi i_{21})(\lambda_{11} - \lambda_{12}) + \theta s_v(i_2 + \phi i_{12})(\lambda_{11} - \lambda_{13}) = 0.$$

This implies

$$u_1 = \frac{M_1}{D_1} = \widetilde{u_1},$$

where,

$$\frac{\partial \mathcal{H}}{\partial u_2} = u_2 D_2 - \eta(1 - s_v)\lambda_{11} - \eta v_1 \lambda_{12} - \eta v_2 \lambda_{13} = 0,$$

gives

$$u_2 = \frac{\eta((1 - s_v)\lambda_{11} + v_1\lambda_{12} + v_2\lambda_{13})}{D_2} = \widetilde{u_2},$$

and,

$$\frac{\partial \mathcal{H}}{\partial u_3} = u_3 D_3 - \rho s_1 \lambda_6 + \rho s_1 \lambda_{10} - \rho s_2 \lambda_7 + \rho s_2 \lambda_{10} = 0,$$

gives

$$u_3 = \frac{(\rho s_1(\lambda_6 - \lambda_{10}) + \rho s_2(\lambda_7 - \lambda_{10}))}{D_3} = \widetilde{u_3},$$

Again, the upper and lower bounds for these controls are 0 and 1 respectively. In detail, $u_1 = u_2 = u_3 = 0$ if $u_1 < 0$, $u_2 < 0$ and $u_3 < 0$, and $u_1 = u_2 = u_3 = 1$ if $\widetilde{u_1} > 1$, $\widetilde{u_2} > 1$ and $\widetilde{u_3} > 1$, otherwise $u_1 = \widetilde{u_1}$, $u_2 = \widetilde{u_2}$ $u_3 = \widetilde{u_3}$. Hence for these controls ${u_1}^*, {u_2}^*, {u_3}^*$ we get the optimum value of the function J.

5. Control theory results

To find the optimal control and the solutions of disease prevalence after the implementation of each control measure, i.e., $(x^*(t), u^*(t))$, we solve the adjoint equations, together with the transversality conditions, and the equation system (4), where $u^*(t) = (u_1^*, u_2^*, u_3^*)$ and $x^*(t)$ are the correspondent trajectories. For this, numerical methods are used with the default parameter values shown in Table 1.

The optimal control solutions of the model (4) were obtained with MATLAB software.

Note that the proposed cost functional includes a weighted sum of several efforts for each specific control measure. The costs are not necessarily quantified as economic costs as the costs for implementing a control measure may vary from region to region experiencing different needs in their public health context as well as different limitations of resources. The costs for each intervention measure can be "low", "medium" or "high", but are assumed to be always less expensive than the cost of infection. The initial value for the weight constants for the human host infections are $A_1 = 1, A_2 = 1, A_3 = 1, A_4 = 1$, while the cost for protection against mosquito bites, reduction of vector abundance and vaccination are $D_1 = 0.3, D_2 = 0.9$ and $D_3 = 0.7$ respectively. The differences in weights were defined using common sense, since the real economical costs are unknown. Moreover, as opposed to most of the already existing optimal control studies applied to vector-borne diseases, the weight constant associated with mosquito infections is fixed to $A_5 = 0$, i.e. there is no cost associated for infection occurring in mosquitoes.

As proposed in [68], the control problem is solved by the forward-backward sweep method, for a time interval of 5 years ($[0, 5]$). The relevant optimal controls are updated using these state and adjoint variables solutions, and these iterative procedures are continued until a predefined convergence threshold is reached. Using numerical simulations, we will investigate three different strategies considering the implementation of a single control measure at the time (Strategy I), the implementation of two control measures simultaneously (Strategy II) and finally, the implementation of those three control strategies together (strategy III).

5.1. Strategy I: Only one control at the time

Strategy one is used to identify which of the available control measure is most effective in reducing the number of disease cases in a period of time. To evaluate the impact of a control measure to reduce transmissibility from vectors to humans and from humans to vectors such as personal protection to avoid mosquito bites (using repellents on skin and clothing, for example), we have implemented a control function $u_1(t)$ to minimize the objective function J, while the control functions $u_2(t) = u_3(t) = 0$ (policy A). The control profile is shown in 5(a) and its effect on the number of severe cases is shown in Figure 5(b).

To evaluate the impact of intervention measures aiming at reducing vector population, such as indoor residual spraying and a combination of interventions to attack the vector at different stages of its life cycle, the control function $\eta u_2(t)$ is implemented to minimize the objective function J, while the other two control measures are $u_1(t) = u_3(t) = 0$ (police B). The control profile is shown in Fig. 5(c), and effect on the number of severe cases is shown in Figure 5(d).

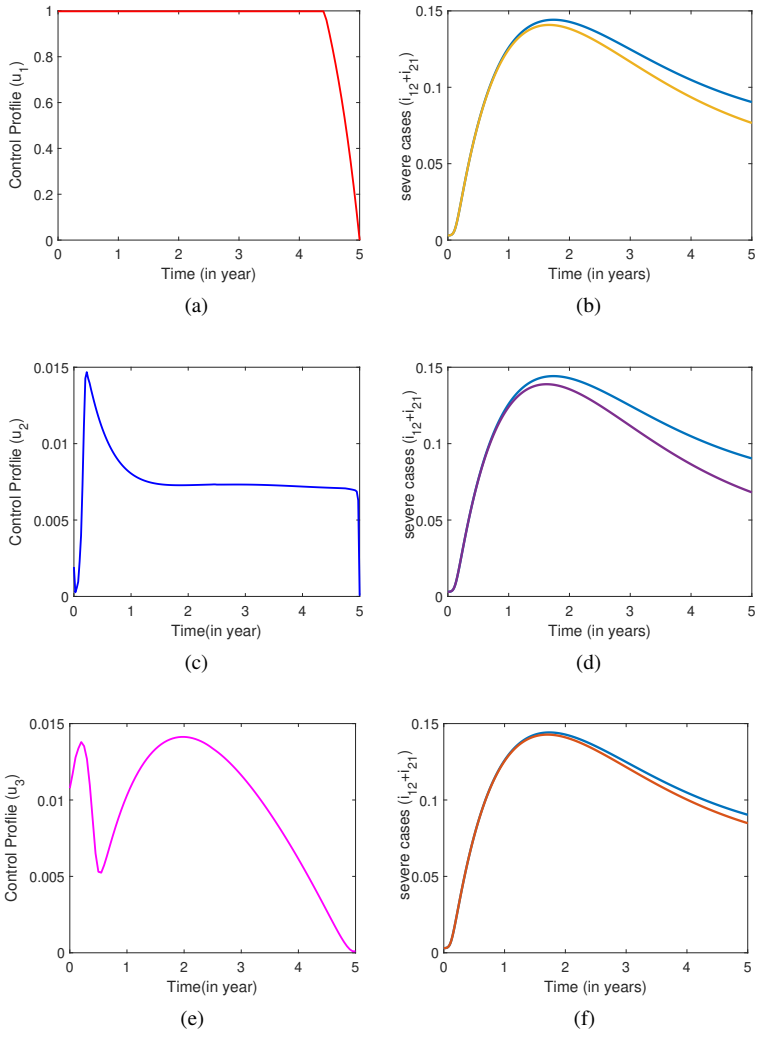

Figure 5: Strategy I: Only one control is used at the time. In (a), (c) and (e), control profiles for $u_1(t)$ (policy A), $u_2(t)$ (policy B) and $u_3(t)$ (policy C), respectively. The effect on the prevalence of severe cases ($i_{12} + i_{21}$) for policy A, policy B and police C over 5 years are shown in (b), (d) and (f) respectively, where blue lines show disease prevalence in the absence of control while lines in yellow, red and purple represent disease prevalence after control implementation.

Finally, to evaluate the effect of vaccination programs restricted to seropositive individuals only, i.e. after a serological screening prior to vaccination, the control function $\rho u_3(t)$ is implemented to minimize the objective function J, while the other possible control interventions are $u_1(t) = u_2(t) = 0$ (policy C). We consider constant vaccine distribution initially set as $\rho = 0.2$. The control profile is shown in Fig. 5(e), and the and effect on the number of severe cases is shown in Figure 5(f).

Over a 5 years period, policy A leads to a moderate reduction of disease cases (approximately 15% and 1.5% for overall infections and severe cases respectively) when the control measure is maintained at its maximum level for the whole time period, while policy B shows the best result in reducing disease cases (approximately 18% and 2% for overall infections and severe cases respectively). Here, control measures for mosquito reduction starts at its maximum level, following a smooth decrease throughout the first year, and are kept at a constant level during the following years. Policy C leads to small reduction of severe cases (approximately 10% and 0.5% for overall infections and severe cases respectively) mostly because it depends on the availability of seropositive individuals to receive the vaccine. Note that on top of that, when evaluation this strategy, one must consider the associated high costs of population screening

prior vaccination which economically speaking might by lead to an even lower cost-effectiveness of this measure. The vaccination control profile shows a peculiar shape, initiated with a rapid increase of vaccine (possibly related to the availability of seropositive individuals) that is quickly relaxed during the first year (possible because of the lack of seropositive individuals in the population). Vaccine distribution gradually increases again (when the target population receiving this vaccine increases) for the following 2 years before its smooth relaxation in the following years.

Overall, within Strategy I, policy B is the most effective policy to be implemented, followed by policy A and policy C.

5.2. Strategy II: Two controls implemented simultaneously

The ability to provide guidance on how best to allocate the often scarce resources while implementing the most cost-effective control strategies will have significant economical consequences of future public health decision making. Strategy II combines the use of two controls simultaneously, aiming to identify which combinations are most effective in reducing the number of infections, enabling a more genuine and realistic assessment of mosquito-borne disease control in the public health context.

We investigate three combinations to minimize the objective function J as follows. (i) the use of personal protection to avoid mosquito bites $u_1(t)$ combined with vector-control program to reduce mosquito population $u_2(t)$ (policy D), (ii) the use of personal protection to avoid mosquito bites $u_1(t)$ combined with vaccination of seropositive individuals only $u_3(t)$ (policy E), and (iii) vaccination of seropositive individuals $u_3(t)$ combined with vector control mosquito program to reduce mosquito population $u_2(t)$ (policy F). The profiles of the possible control measure combination are shown in Fig.6.

Over 5 years period, policy D leads to a significant reduction of cases (approximately 24% and 5% for overall infections and severe cases respectively) when personal protection to avoid mosquito bites ($u_1(t)$) is maintained at its highest level for the first 3.5 years, together with measures to control vector abundance ($u_2(t)$) applied initially at its maximum level, gradually decreasing up to a constant level, see Fig. 6(c). Policy E leads to a slightly smaller reduction on disease cases (approximately 22% and 3% for overall infections and severe cases respectively) when protection against mosquito bites is kept at its maximum level for 3 consecutive years before being relaxed, combined with vaccine distribution with a similar shape as observed for police C, with slightly less effort during the second phase of the control implementation, see Fig. 6(f). Policy F leads to a similar reduction of disease cases (approximately 23% and 4% for overall infections and severe cases respectively) with control u_3 and control u_2 being implemented as proposed for police D and police E respectively, see Fig. 6(i). Overall, within Strategy II, policy D is the most effective policy to be implemented, followed by policy F and policy E.

5.3. Strategy III: Three controls implemented simultaneously

Strategy III combines the use of all three control measures $u_1(t)$, $u_2(t)$ and $u_3(t)$ simultaneously (policy G). The control profiles are shown in Fig.7(a-c) for $u_1(t)$, $u_2(t)$ and $u_3(t)$, respectively. Surprisingly, police G leads to a similar results as obtained with Strategy II, policy D, able to reduce, over a period of 5 years, the number of overall infections by approximately 26% and only 5% for severe cases. Here, while protection against mosquito bites $u_1(t)$ can be relaxed after 2 years, the program to reduce mosquito population $u_2(t)$ must be kept at its highest level throughout the time, combined with vaccine distribution $u_3(t)$ following a similar control profile as shown for Strategy II, see Fig. 7.
The comparison of the performance of public health strategies for reducing dengue infections is shown in Figure 8.

5.4. The effect of weight constant values on policies and model limitations

Aiming at finding a solution that minimizes the cost functions, we define a weight constant (cost) for each control measure, based on a common sense and realistic information, giving the final solution for an optimized strategy. While the optimal control solutions are bound to the assigned weight constants, here we vary the initial weight constant values to explore the variation on the results, see Fig. 9(a), Fig. 9(b) and Fig. 9(c) for u_1, u_2 and u_3 respectively. This exploratory analysis allows us to investigate the impact of various costs for a control measure. For these combinations, the qualitative results are consistent in respect to the best policy for disease control, while different weights will change the final quantitative results for disease prevalence, increasing or decreasing the number of infections over a period of 5 years, see Fig. 9(d-f) and Fig. 9(g-i) for overall infections and severe cases respectively.

5.5. The impact of vaccine distribution rate (ρ) and the additional killing mosquito factor (η)

Similarly to the analysis performed in Section 5.4, the vaccine distribution ρ and the additional killing mosquito η factors are varied to explore their impact on disease control performance.

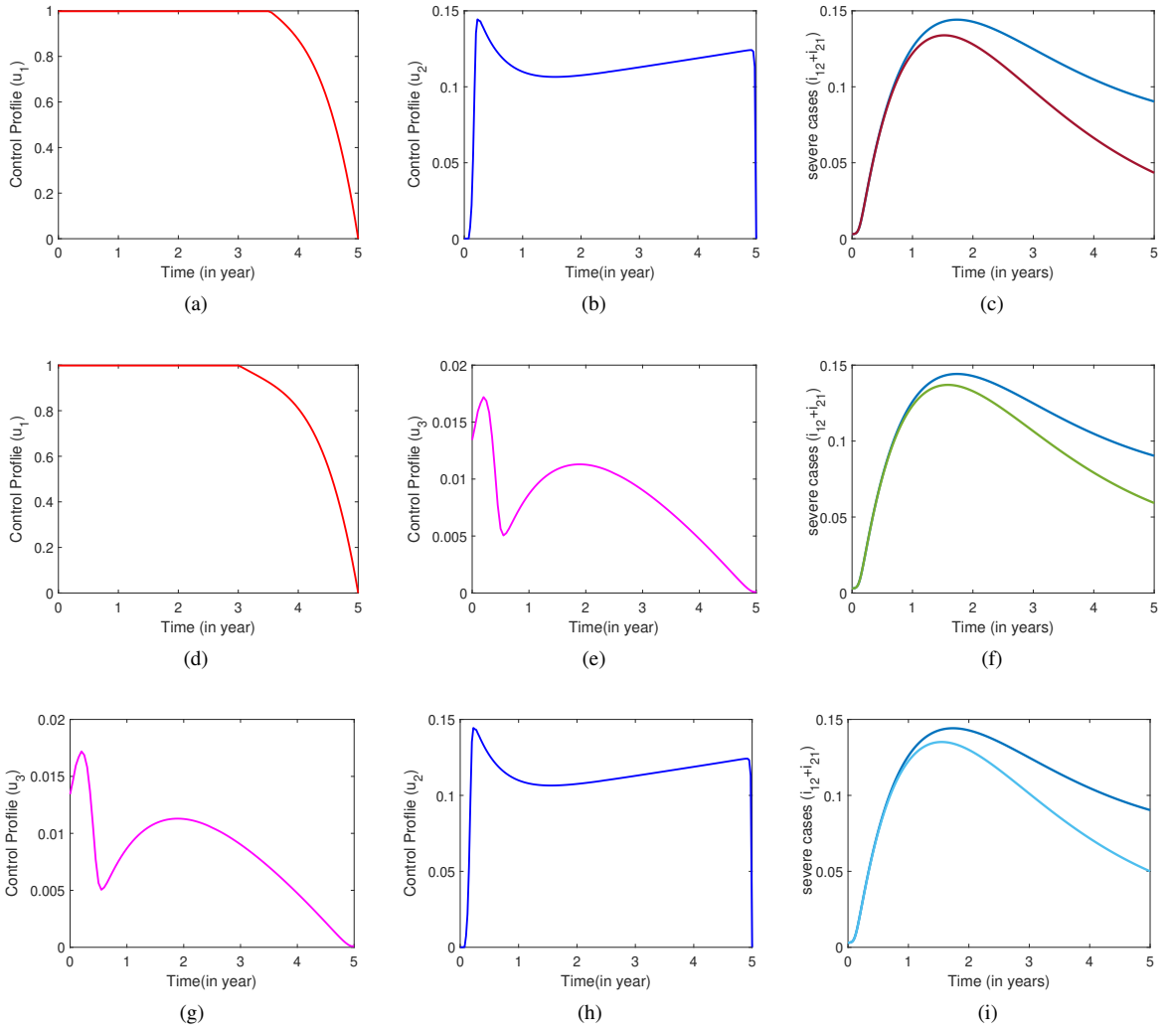

Figure 6: Strategy II: Two control measures are used simultaneously. In (a) the control profile for the $u_1(t)$ and in (b) the control profile for the $u_2(t)$ (policy D). In (d) the control profile for the u_1 and in (e) the control profile for the u_3 (policy E). In (g) the control profile for the $u_2(t)$ and in (h) the control profile for the u_3 (policy F). Reduction of severe dengue infections $(i_{12}+i_{21})$ for policy D, policy E and policy F are shown in (c), (f) and (i) respectively, where the blue line refers to disease prevalence in the absence of control and the lines in green, brown and cyan represent disease prevalence after the combined controls are implemented over a period of 5 years.

Figure 10(a) and (b) show the impact of various values of vaccine distribution factor (see color lines) on overall cases and severe cases respectively. Note that although vaccination is restricted to seropositive individuals only, we have a strong assumption of a perfect vaccine, i.e. 100% vaccine efficacy, being initially distributed to given percentage of seropositive individuals per year. Here, the parameter ρ is used as proxy for vaccination coverage and results change when different vaccine efficacy is considered. Overall, if the cost for vaccine distribution decreases, a small reduction of severe cases (up to 1.4%) and a moderate reduction of overall infections (up to 11%), are observed.

Figure 10(c) and (d) show the impact of various values of additional killing mosquito factor (see color lines) on overall cases and severe cases respectively. In respect to the effectiveness of vector control programs, the additional killing mosquito factor leads to a moderate reduction of severe cases (up to 3.3%) and higher reduction of overall infections (up to 22%) when the costs decreases.

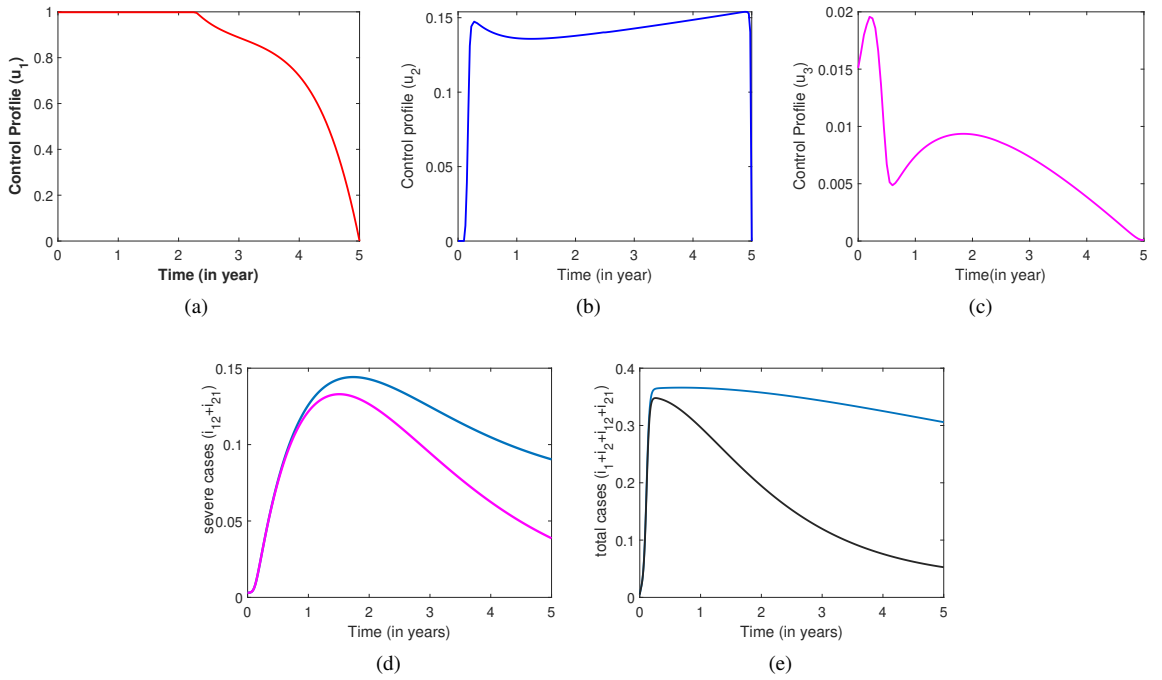

Figure 7: Strategy III: Three control measures are used simultaneously. In (a) the control profile for the $u_1(t)$, in (b) the control profile for the $u_2(t)$ and in (c) the control profile for the $u_3(t)$. Reduction of severe dengue infections $(i_{12} + i_{21})$ are shown in (d) where the blue line refers to disease prevalence in the absence of control and the pink line represents disease prevalence after the simultaneously implementation of control measures and Reduction of total dengue infections $(i_1 + i_2 + i_{12} + i_{21})$ are shown in (e) where the blue line refers to disease prevalence in the absence of control and the black line represents disease prevalence after the simultaneously implementation of control measures over a period of 5 years.

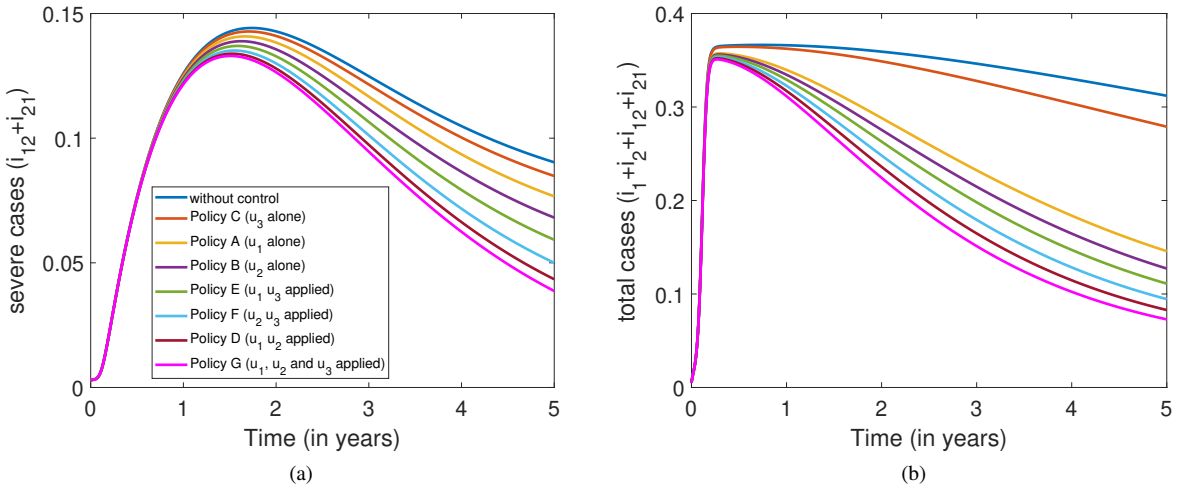

Figure 8: Comparison of the performance of public health strategies in a period of 5 years. Reduction of severe dengue infections $(i_{12} + i_{21})$ and overall disease prevalence $(i_1 + i_2 + i_{12} + i_{21})$ are shown in (a) and (b) respectively.

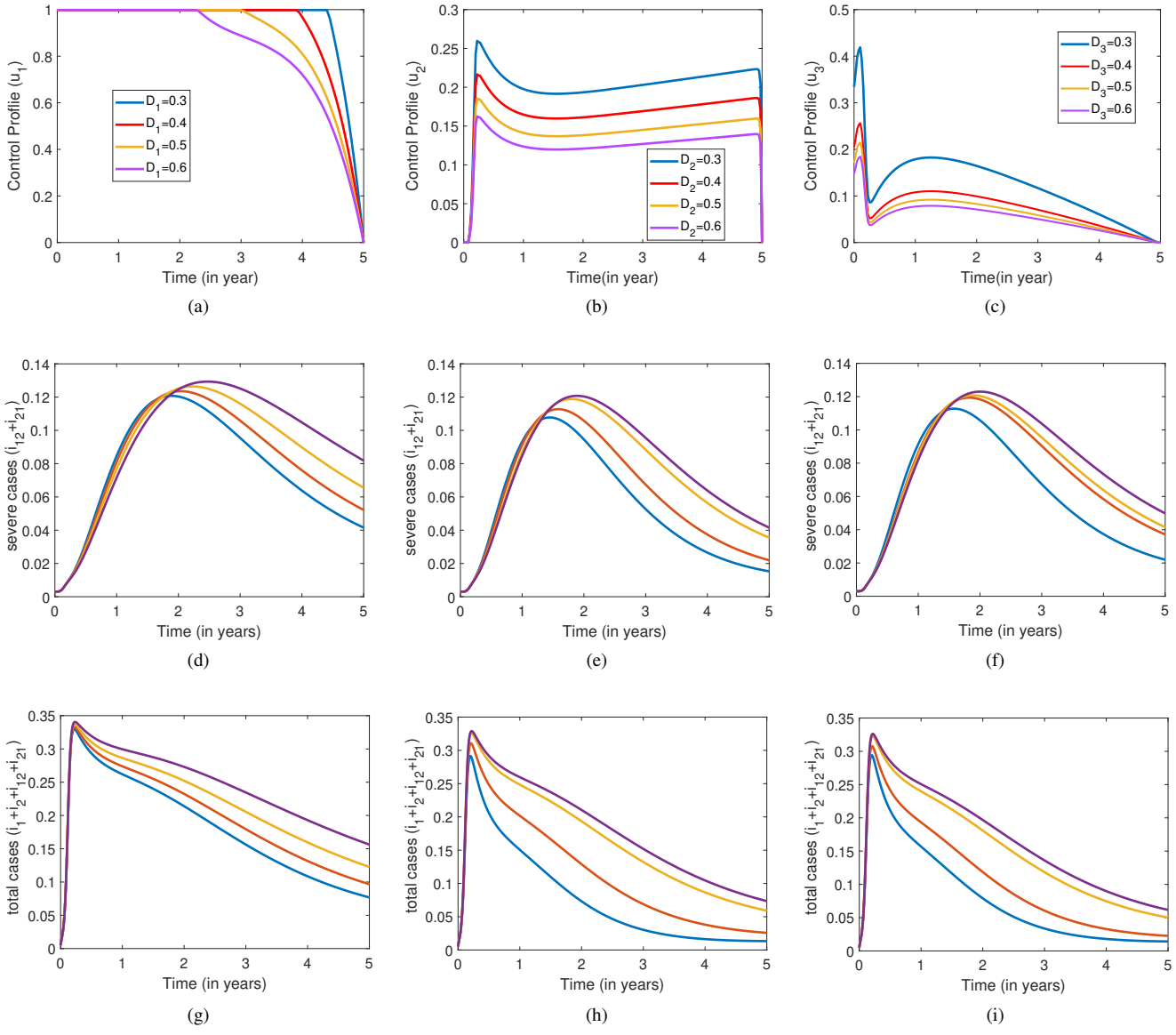

Figure 9: Optimal control profiles with different weigh values and their outcome on disease prevalence. The weight values of a specific control measure is varied and shown in different color lines, while keeping the others fixed to its baseline value shown in Table 1. In (a) the control profile u_1 with various weight for its cost D_1. The effect on overall cases and severe cases are shown in (d) and (g) respectively. In (b) the control profile u_2 with various weight for its cost D_2. The effect on overall cases and severe cases are shown in (e) and (h) respectively. In (c) the control profile u_3 with various weight for its cost D_3. The effect on overall cases and severe cases are shown in (f) and (i) respectively.

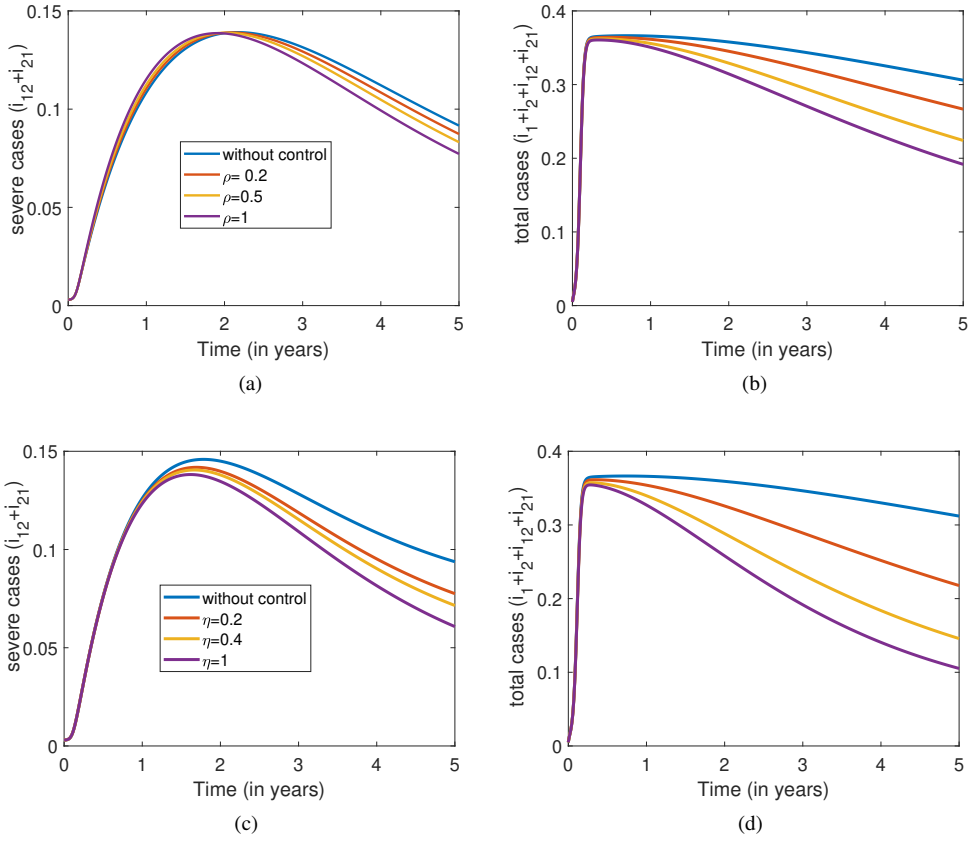

Figure 10: The impact of vaccine distribution rate (ρ) and the additional killing mosquito (η) factor on the prevalence of severe cases ($i_{12} + i_{21}$) and overall cases ($i_1 + i_2 + i_{12} + i_{21}$). Blue lines refer to disease prevalence in the absence of control while the red, yellow and purple lines show the results for various values of the additional factors set to 0.2 (in red), 0.5 (in yellow) and 1 (in purple).

6. Discussions and conclusions

We propose refined vector-host dengue model with strain structure of pathogens including two biological features of dengue fever epidemiology. To determine the key parameters of the model affecting disease transmission, a detailed sensitivity analysis was performed. With these results at hand, the system was extended to include realistic control measures. Using optimal control theory we have evaluated the effect of different strategies for disease control, alone and combined, on severe disease cases and on the overall infections over a period of 5 years.

The optimal control problem studied here considers realistic intervention measures in the public health context. The preventive measures included into the model are: (1) reduction of disease transmission from human to vectors and from vectors to humans by avoiding mosquito bites, (2) reduction of mosquito population by an effective vector control program and (3) vaccination of seropositive individuals, following the current recommendation of the WHO. For each measure, a control function $u_i(t)$ is incorporated to minimize the objective cost function $\boldsymbol{J}$, which includes a weighted sum of several efforts for the controls. Note that the assigned weights for each control measure are not necessarily quantified as economic costs, assuming that the costs for implementing an intervention measure may vary from region to region experiencing different needs in terms of public health burdens, as well as different limitations of resources. In this context, the exploratory analysis performed here allows us to interpret our results in a more realistic way, assuming different scenarios, often neglected by theoretical studies. The control system is analyzed using the Pontryagin‘s Principle for optimal control where three different strategies are compared.

Using numerical simulations we observe that model performance improves when introducing controls, with different outputs observed for different policies, see Fig. 8. In detail, Strategy III, considering the simultaneous use of all three controls, has a higher impact, reducing, over a period of 5 years, approximately 26% and 5% of overall infections and severe cases respectively (see Fig. 7. Strategy II, considering the simultaneous use of two controls together have show a moderate impact on disease prevalence for all the three possible policies. Among them, policy D, combining protection against mosquito bites and reduction of mosquito population, has shown the best performance, reducing approximately 24% and 5% of overall infections and severe cases respectively, followed by policy C and policy A with a slightly less reductions, see Fig. 6. Out of surprise, Strategy I, considering the use of a single control at the time, shows the lowest reductions when compared with the other strategies. Within the three possible policies, policy B has the best performance, reducing approximately 18% and 2% of overall infections and severe cases respectively, followed by policy A and policy C, see Fig. 5. While the optimal control solutions are bound to the assigned weight constants, we have conducted an exploratory analysis for different values of each weight constant, see Fig. 9. Our findings have shown that the assigned costs for the controls were not crucial for the obtained results in respect to the performance of each strategy and its policies, only affecting slightly the quantitative results.

Although these strategies are optimized in term of cost-effectiveness, it is important to mention that in the public health context the real economic costs for control measure implementation are often not publicly available and eventually significantly different from region to region. This is definitely a limitation of the existing optimal control analysis where the economic cost function are not included. Moreover, while resource limitation for public health interventions is a global issue, the economic capacity is significantly different between low and high income countries, without mentioning the specific needs of each region in terms of their current epidemiological scenario. That was observed during the COVID-19 pandemic and it is no different for any other public health burden.

Studies like this can provide important results obtained from numerical experiments (where the weight constants are used as arbitrary values and will influence the outcomes), however, we claim that using the common sense while assigning "realistic" differences for the weights of an specific control is fundamental to a correct interpretation and eventual extrapolation of the results into a real world problem.

Specific for this study, we have assumed a very low cost for self-preventive measure ($D_1 = 0.3$) as they are often bought by the individuals themselves without much financial effort from the public health decision making (governmental) view point. On the other hand, we have assumed a very high cost for vector control programs to reduce mosquito population ($D_2 = 0.9$), and a slightly smaller cost for vaccinating seropositive individuals only ($D_2 = 0.7$). This assumption is justified when vector control programmes are widely implemented worldwide, covering large geographic scales, while vaccination is only recently available and restricted to specific target groups (seropositives) existing only in endemic countries. Note that the extra effort of human resources to perform population screening prior to vaccination is not considered as incremental cost. While the simultaneous use of controls are highly effective, the use of a single control measure can eventually produce similar effects on disease prevalence as shown in our study. We propose a careful evaluation of the epidemiological scenario before designing strategies for disease prevention and

control, as that would allow an optimal allocation of the public health resources considering the specific needs of each region.

Acknowledgment

Akhil Kumar Srivastav acknowledge the financial support by the Ministerio de Ciencia e Innovación (MICINN) of the Spanish Government through the Juan de la Cierva Formación grant FJC2021-046826-I. We would like to thank Bob W. Kooi, Vrije Universiteit Amsterdam for fruitful discussions.

Funding Statement

M. A. has received funding from the European Union's Horizon 2020 research and innovation programme under the Marie Skłodowska-Curie grant agreement No 792494. This research is also supported by the Basque Government through BERC 2022-2025 program, and by the Spanish Ministry of Sciences, Innovation and Universities: BCAM Severo Ochoa accreditation CEX2021-001142-S / MICIN / AEI / 10.13039/501100011033.

Appendix

(I) Basic Reproduction Number $\mathcal{R}_0$ calculations

The basic reproduction number, R_0, of the system (3), is calculated using the next generation matrix method [70]. The compartmental model is decomposed into $\mathcal{F}$ and $\mathcal{V}$ as follows:

$$\mathcal{F} = \begin{pmatrix} \beta s v_1 \\ \beta s v_2 \\ \beta s_1 v_2 \\ \beta s_2 v_1 \\ \theta s_v(i_1 + \phi i_{21}) \\ \theta s_v(i_2 + \phi i_{12}) \end{pmatrix} \qquad \textit{and} \qquad -\mathcal{V} = \begin{pmatrix} \\ (\gamma+\mu)i_1 \\ (\gamma+\mu)i_1 \\ (\gamma+\mu)i_{12} \\ (\gamma+\mu)i_{21} \\ \nu v_1 \\ \nu v_2 \end{pmatrix}.$$

Considering F the Jacobian matrix of $\mathcal{F}$ at the disease free equilibrium E_0,

$$F = \begin{pmatrix} 0 & 0 & 0 & 0 & \beta & 0 \\ 0 & 0 & 0 & 0 & 0 & \beta \\ 0 & 0 & 0 & 0 & 0 & 0 \\ 0 & 0 & 0 & 0 & 0 & 0 \\ \theta & 0 & 0 & \theta\phi & 0 & 0 \\ 0 & \theta & \theta\phi & 0 & 0 & 0 \end{pmatrix}$$

and V, the Jacobian matrix of $\mathcal{V}$ at E_0,

$$V = \begin{pmatrix} (\gamma+\mu) & 0 & 0 & 0 & 0 & 0 \\ 0 & (\gamma+\mu) & 0 & 0 & 0 & 0 \\ 0 & 0 & (\gamma+\mu) & 0 & 0 & 0 \\ 0 & 0 & 0 & (\gamma+\mu) & 0 & 0 \\ 0 & 0 & 0 & 0 & \nu & 0 \\ 0 & 0 & 0 & 0 & 0 & \nu \end{pmatrix}$$

the next generation matrix $K = FV^{-1}$ has a non-negative eigenvalue, with $\mathcal{R}_0$ being the greatest eigenvalue, in modulus, of K [70] .

The eigenvalues are given explicitly by

$$Eig(K) = \left(0, 0, \sqrt{\frac{\theta\beta}{\nu(\gamma+\mu)}}, \sqrt{\frac{\theta\beta}{\nu(\gamma+\mu)}}, -\sqrt{\frac{\theta\beta}{\nu(\gamma+\mu)}}, -\sqrt{\frac{\theta\beta}{\nu(\gamma+\mu)}}\right)$$

$$\mathcal{R}_0 = \sqrt{\frac{\theta\beta}{\nu(\gamma+\mu)}}.$$

(II) The role of disease enhancement factor ϕ via the ADE process

The value of the disease enhancement factor ϕ can be tuned to reflect different situations. A value of $\phi > 1$ describes the scenario where secondary infections (severe cases) have larger infectivity than primary infections (mild cases), due to the enhanced viral load (via the ADE process) leading to hospitalization and hence, decreasing the mobility and interactions with mosquitoes. On the other hand, $\phi < 1$ describes the scenario whereas primary infections contribute more to the force of infection (than the secondary infections), due to their higher mobility and possibility of interaction with mosquitoes [4, 30–33, 48, 49].

The main results of this work are obtained for $\phi < 1$. Here, we present the effect of this parameter on the model time series output.

In detail, for the scenario of $\phi < 1$, see Fig. 11(a-c), as the parameter value increases the solution of the system changes from stable equilibria to stable periodic solutions. Figure 11 (a) shows that solutions converge to endemic

equilibria, (b) to a stable periodic solution, (c) and (d) to a double limit cycle. On the other hand, for the scenario of $\phi > 1$, see Fig. 12, there is no change of the behaviour of the system as the parameter increases, with all the solutions converging to periodic solutions. In addition, as ϕ increase the prevalence of the total infection also increases.

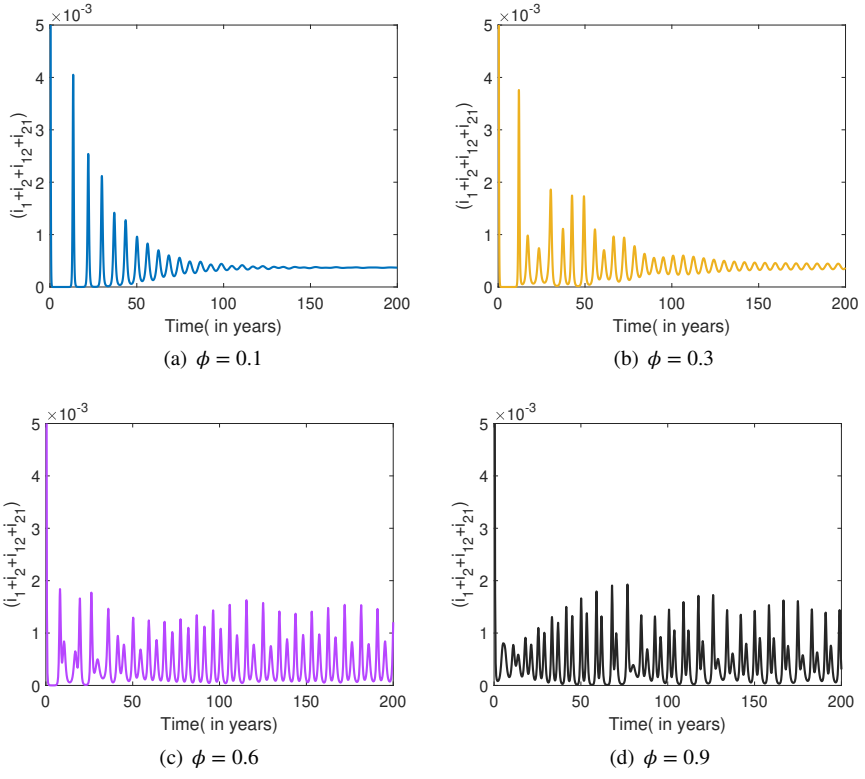

Figure 11: Time series for $\phi < 1$. The other parameters are fixed as described in Table 1. In (a) $\phi = 0.1$, in (b) $\phi = 0.3$, in (c) $\phi = 0.6$, and in (d) $\phi = 0.9$.

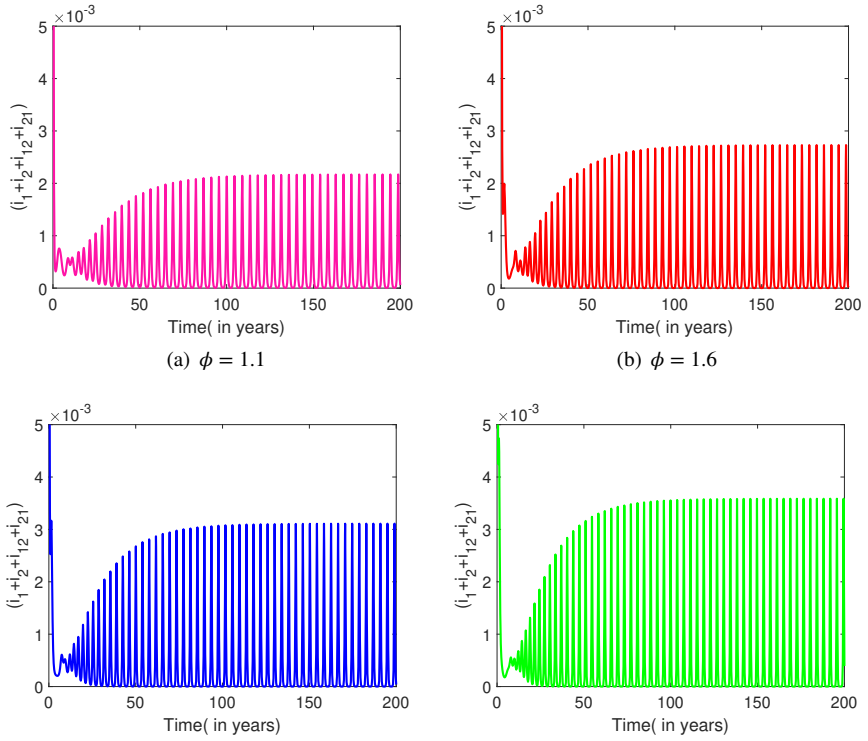

(a) $\phi = 1.1$ (b) $\phi = 1.6$

(c) $\phi = 2$ (d) $\phi = 2.6$

Figure 12: Time series considering scenario $\phi > 1$, for the parameter set $\beta = 2 * \gamma,\ \gamma = 52,\ \theta = 73, \mu = (1/65)$, and $\alpha = 2$. Fig. (a) $\phi = 1.1$, (b) $\phi = 1.6$, (c) $\phi = 2$, and (d) $\phi = 2.6$. Baseline values of parameters are described in Table 1.

Figure 13 shows the long term behaviour of the time series solution and the respective phase space plots in one and in two dimensions for the scenario of $\phi < 1$, while Figure 14 shows the long term behaviour of the time series solution and the respective phase space plots in two dimensions (2d) and in three dimensions (3d) for the scenario of $\phi > 1$.

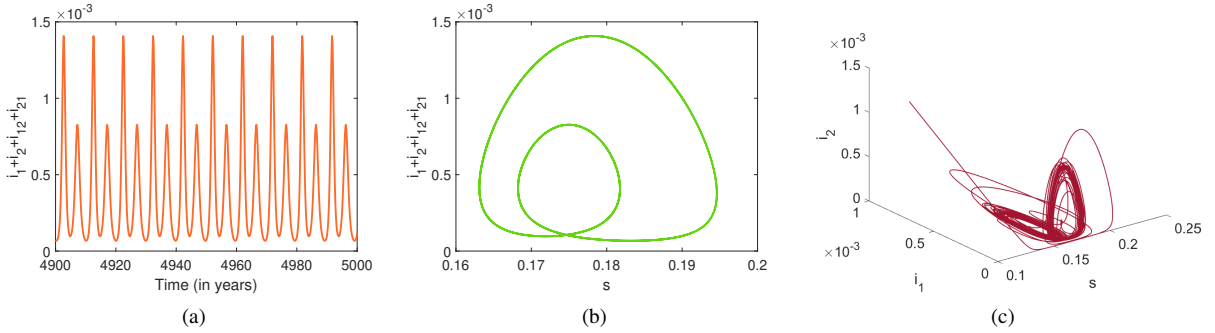

Figure 13: With 5000 years of transients discarded, in (a) time series for $\phi = 0.6$, in (b) the 2d phase plot showing the double limit cycle attractor. In (c) the 3d phase plot considering the variables s, i_1 and i_2. Baseline parameter values are shown in Table 1.

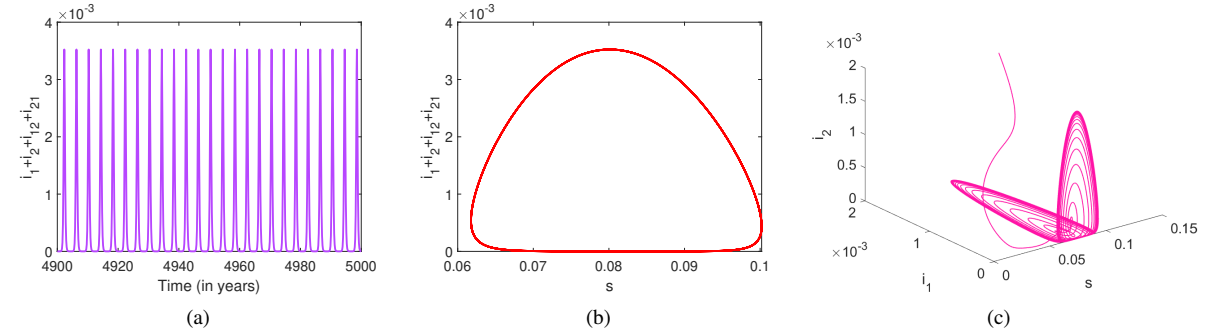

Figure 14: With 5000 years of transients discarded, in (a) time series for $\phi = 2.6$, in (b) the 2d phase plot showing the double limit cycle attractor. In (c) the 3d phase plot considering the variables s, i_1 and i_2. Baseline parameter values are shown in Table 1.

We observe the clear switch from a double limit cycle (see Fig. 13) to a single limit cycle (see Fig. 14) as ϕ increases.

(III) The role of temporary cross-immunity α

The main results of this work are obtained for the disease enhancement factor $\phi < 1$ and intermediate temporary cross immunity period $\alpha = 2$. Here, we present the effect of different temporary cross immunity periods, from long to small, on the model time series output for the scenarios of $\phi < 1$, see Figure 15, and of $\phi > 1$, see Figure 16.

For the scenario of $\phi < 1$, see Fig. 15, as the parameter α increases, from $\alpha = 2$, representing an intermediate temporary cross immunity period (6 months), to $\alpha = 52$, representing a negligible temporary cross immunity period (7 days), the solutions of the system change from stable double limit cycle to stable equilibrium solution. For the scenario of $\phi > 1$, see Fig. 16, as the parameter α increases, the solutions of the system change. Stable single limit cycles are observed for $\alpha = 2$ and $\alpha = 32$), while a complex attractor is observed for $\alpha = 12$, followed by a stable equilibrium solution $\alpha = 52$.

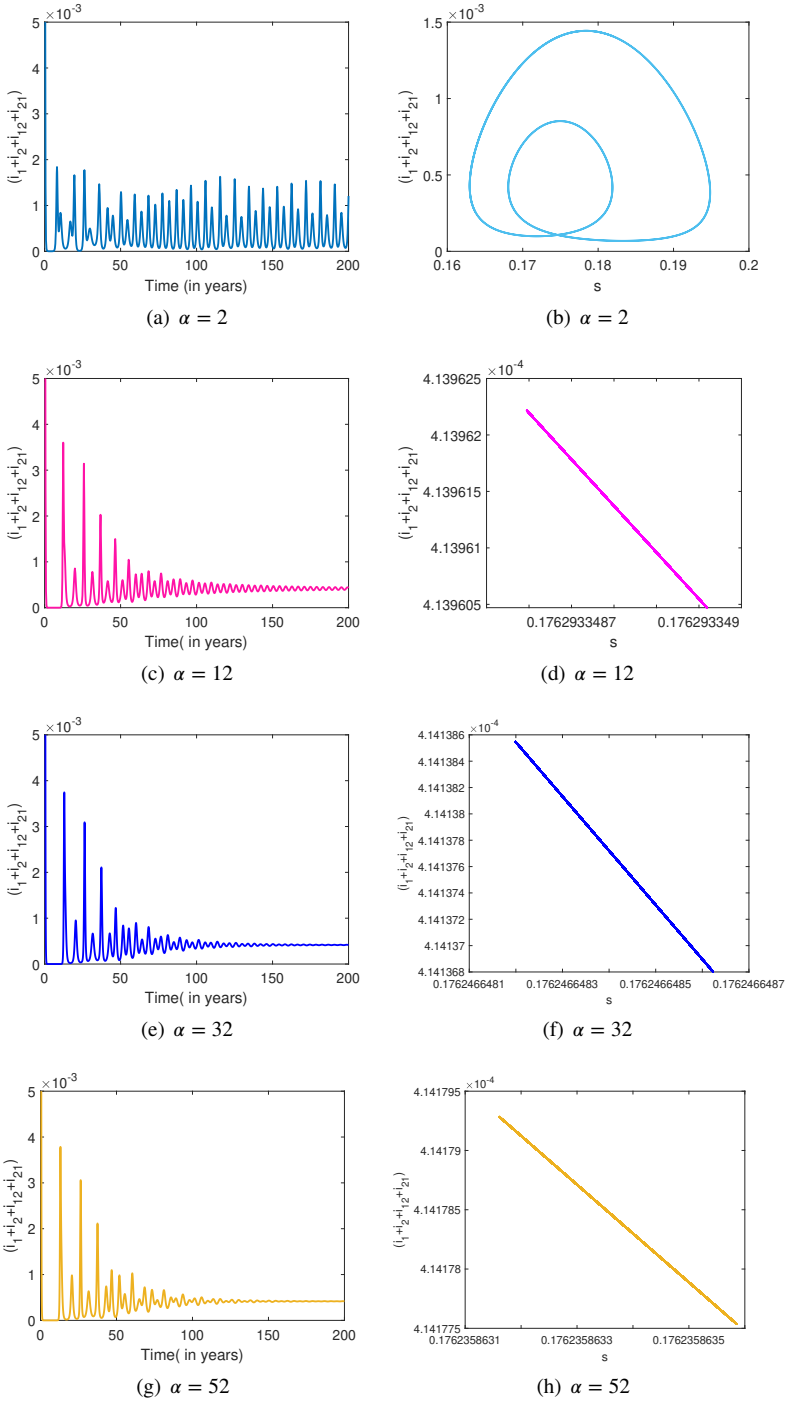

Figure 15: Time series and state space for fixed $\phi = 0.6$. Baseline parameter values are shown in Table 1. In (a-b) $\alpha = 2$, in (c-d) $\alpha = 12$, in (e-f) $\alpha = 32$, and in (g-h) $\alpha = 52$.

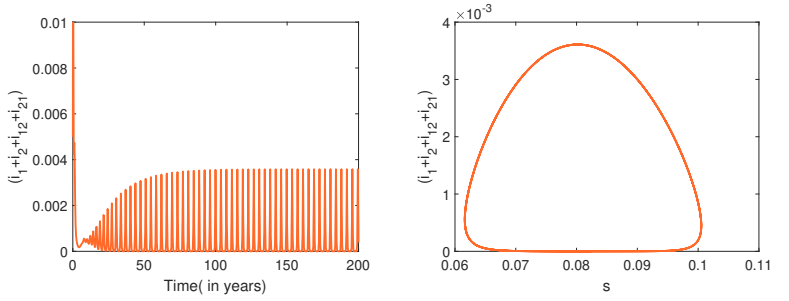

(a) $\alpha = 2$

(b) $\alpha = 2$

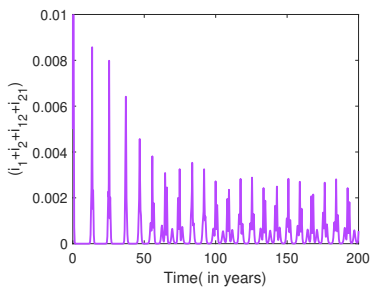

(c) $\alpha = 12$

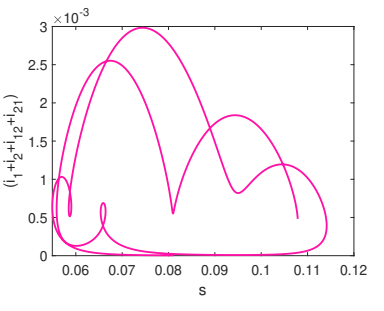

(d) $\alpha = 12$

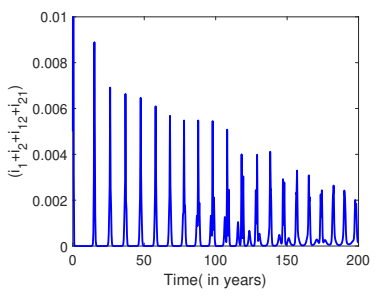

(e) $\alpha = 32$

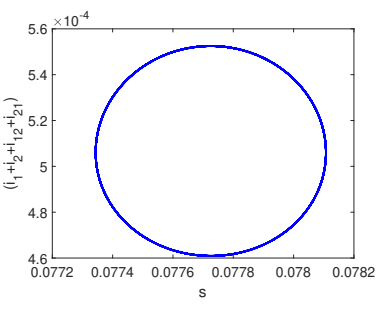

(f) $\alpha = 32$

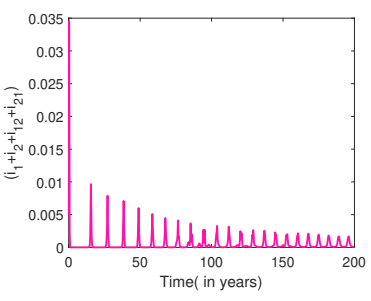

(g) $\alpha = 52$

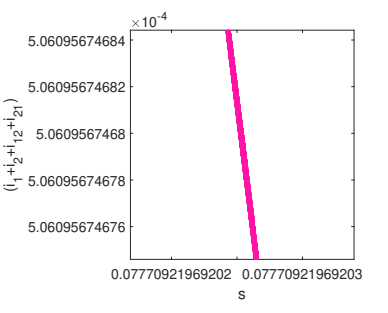

(h) $\alpha = 52$

Figure 16: Time series and state space for fixed $\phi = 2.6$. Baseline parameter values are shown in Table 1. In (a-b) $\alpha = 2$, in (c-d) $\alpha = 12$, in (e-f) $\alpha = 32$, and in (g-h) $\alpha = 52$.

(IV) The impact of implementing control measures for longer period of time

While the main results of this work evaluates the results of disease cases after five years of control implementation, here we explore the effect of longer time periods on overall disease prevalence, see Fig. 17(a) and (c) for the scenario of $\phi < 1$, Fig. 17 (b) and (d) for the scenario of $\phi > 1$.

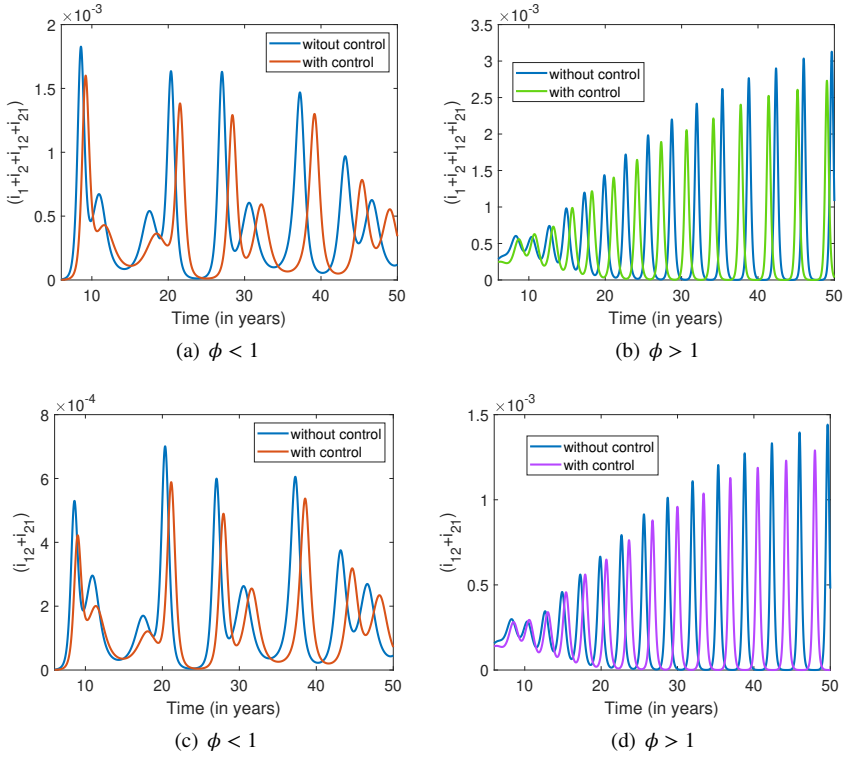

Figure 17: Prevalence of infections in the human population when all control measures (policy G) are applied for longer time period (50 years). For $phi < 1$: (a) overall infections $(i_1 + i_2 + i_{12} + i_{21})$, and in (b) severe cases $(i_{12} + i_{21})$. For $phi > 1$: (c) overall infections $(i_1 + i_2 + i_{12} + i_{21})$, and in (d) severe cases $(i_{12} + i_{21})$. Baseline parameter values are shown in Table 1.

Here we observe that applying the control measures for longer period will shift and decrease the burden of the outbreaks, however, this strategy is also not able to eradicate the disease. For longer time simulations, the final outcome for $\phi < 1$ is a double limit cycle wheres for $\phi > 1$ a single limit cycle is observed.

References

[1] I. G. Ameen, D. Baleanu, H. M. Ali, An efficient algorithm for solving the fractional optimal control of sirv epidemic model with a combination of vaccination and treatment, Chaos, Solitons Fractals 137 (2020) 112699.

[2] A. M. V. A. J. Dumitru Baleanu, Manijeh Hasanabadi, A new intervention strategy for an hiv/aids transmission by a general fractional modeling and an optimal control approach, Chaos, Solitons Fractals 167 (2023) 111197.

[3] K. Blayneh, Y. Cao, H.-D. Kwon, Optimal control of vector-borne diseases: Treatment and prevention, Discrete and Continuous Dynamical Systems - Series B (DCDS-B) 11 (2009) 587–611.

[4] M. Aguiar, S. Ballesteros, B. W. Kooi, N. Stollenwerk, The role of seasonality and import in a minimalistic multi-strain dengue model capturing differences between primary and secondary infections: Complex dynamics and its implications for data analysis, J Theor Biol 289 (2011) 181–196.

[5] S. B. Halstead, Dengue hemorrhagic fever: two infections and antibody dependent enhancement, a brief history and personal memoir, Rev Cubana Med Trop 54 (2002) 171–179.

[6] S. B. Halstead, Neutralization and antibody-dependent enhancement of dengue viruses, Adv Virus Res 60 (2003) 421–467.

[7] M. G. Guzman, S. B. Halstead, H. Artsob, et al., Dengue: a continuing global threat, Nature reviews microbiology 8(12) (2010) S7–S16.

[8] W. Dejnirattisai, A. Jumnainsong, N. Onsirisakul, P. Fitton, S. Vasanawathana, et al., Cross-reacting antibodies enhance dengue virus infection in humans, Science 328(5979) (2010) 745–748.

[9] W. Dejnirattisai, P. Supasa, W. Wongwiwat, A. Rouvinski, G. Barba-Spaeth, T. Duangchinda, et al., Dengue virus sero-cross-reactivity drives antibody-dependent enhancement of infection with zika virus., Nature immunology 17(9) (2016) 1102–1108.

[10] L. C. Katzelnick, L. Gresh, M. E. Halloran, J. C. Mercado, G. Kuan, A. Gordon, A. Balmaseda, E. Harris, Antibody-dependent enhancement of severe dengue disease in humans., Science 358(6365) (2017) 929–932.

[11] O. J. Brady, P. W. Gething, S. Bhatt, J. P. Messina, J. S. Brownstein, et al., Refining the global spatial limits of dengue virus transmission by evidence-based consensus., PLOS Neglected Tropical Diseases 6(8) (2012) e1760.

[12] S. Bhatt, P. W. Gething, O. J. Brady, J. P. Messina, A. W. Farlow, C. L. Moyes, J. M. D. et al., The global distribution and burden of dengue, Nature 496 (2013) 504–507.

[13] W. H. O. WHO, World health organization. accessed in may 2022, https://www.who.int/news-room/fact-sheets/detail/dengue-and-severe-dengue, 2022.

[14] S. R. Hadinegoro, J. L. Arredondo-García, M. R. Capeding, et al., Efficacy and long term safety of a dengue vaccine in regions of endemic disease, New England Journal of Medicine 373 (2015) 1995–1206.

[15] S. Biswal, H. Reynales, X. Saez-Llorens, P. Lopez, et al., Efficacy of a tetravalent dengue vaccine in healthy children and adolescents., N. Engl. J. Med. 381 (2019) 2009–2019.

[16] S. Biswal, C. Borja-Tabora, L. M. Vargas, H. Velásquez, M. T. Alera, V. Sierra, et al., Efficacy of a tetravalent dengue vaccine in healthy children aged 4–16 years: A randomised, placebo-controlled, phase 3 trial., Lancent 381 (2019) 1423–1433.

[17] M. Aguiar, N. Stollenwerk, S. B. Halstead, The Risks behind Dengvaxia Recommendation, The Lancet Infectious Diseases 16 (2016) 882–883.

[18] S. B. Halstead, M. Aguiar, Dengue vaccines: Are they safe for travelers?, Travel Med Infect Dis 14(4) (2016) 378–383.

[19] M. Aguiar, S. B. Halstead, N. Stollenwerk, Consider stopping dengvaxia administration without immunological screening, Expert Review of Vaccines 16(4) (2017) 301–302.

[20] M. Aguiar, N. Stollenwerk, Dengvaxia: Age as surrogate for serostatus, Lancet Infect. 18 (2018) 245.

[21] M. Aguiar, N. Stollenwerk, Dengvaxia efficacy dependency on serostatus: A closer look at more recent data., Clin. Infect. Dis. 66 (2018) 641–642.

[22] W. M. P. B. Wahala, A. M. de Silva, The human antibody response to dengue virus infection, Viruses 66 (2011) 2374–2395.

[23] M. Aguiar, N. Stollenwerk, The impact of serotype cross-protection on vaccine trials: Denvax as a case study, Vaccines 8 (2020) 674.

[24] L. J. White, E. F. Young, M. J. Stoops, S. R. Henein, E. C. Adams, R. S. Baric, A. M. de Silva, Defining levels of dengue virus serotype-specific neutralizing antibodies induced by a live attenuated tetravalent dengue vaccine (tak-003), PLoS Negl. Trop. Dis. 15 (2021) e0009258.

[25] L. Rivera, S. Biswal, X. Sáez-Llorens, H. Reynales, E. López-Medina, C. Borja-Tabora, L. Bravo, C. Sirivichayakul, P. Kosalaraksa, L. M. Vargas, D. Yu, V. Watanaveeradej, F. Espinoza, R. Dietze, L. Fernando, P. Wickramasinghe, E. D. MoreiraJr, A. D. Fernando, D. Gunasekera, K. Luz, R. V. Cunha, M. Rauscher, O. Zent, M. Liu, E. Hoffman, I. LeFevre, V. Tricou, D. Wallace, M. Alera, A. Borkowski, Three-year Efficacy and Safety of Takeda's Dengue Vaccine Candidate (TAK-003), Clinical Infectious Diseases 75 (2022) 107–117.

[26] D. B. Fischer, S. B. Halstead, Observations related to pathogenesis of dengue hemorrhagic fever. V. Examination of agspecific sequential infection rates using a mathematical model, The Yale journal of biology and medicine 42 (1970) 329–349.

[27] M. Aguiar, V. Anam, K. B. Blyuss, C. D. S. Estadilla, B. V. Guerrero, D. Knopoff, B. W. Kooi, A. K. Srivastav, V. Steindorf, N. Stollenwerk, Mathematical models for dengue fever epidemiology: A 10-year systematic review, Physics of Life Reviews 40 (2022) 65–92.

[28] A. A. Sebayang, H. Fahlena, V. Anam, D. Knopoff, N. Stollenwerk, M. Aguiar, E. Soewono, Modeling dengue immune responses mediated by antibodies: A qualitative study, Computational and Mathematical Methods 941 (2021) 10.

[29] V. Anam, A. A. Sebayang, H. Fahlena, D. Knopoff, N. Stollenwerk, E. Soewono, M. Aguiar, Modeling dengue immune responses mediated by antibodies: Insights on the biological parameters to describe dengue infections, Computational and Mathematical Methods 2022 (2022) 11.

[30] M. Aguiar, B. W. Kooi, F. Rocha, P. Ghaffari, N. Stollenwerk, How much complexity is needed to describe the fluctuations observed in dengue hemorrhagic fever incidence data?, Ecological Complexity 16 (2013) 31–40.

[31] M. Aguiar, B. W. Kooi, N. Stollenwerk, Multi-strain deterministic chaos in dengue epidemiology, a challenge for computational mathematics, AIP Conference Proceedings 1168 (2009) 1555.

[32] M. Aguiar, S. Ballesteros, N. Stollenwerk, Two strain dengue model with temporary cross immunity and seasonality, AIP Conference Proceedings 1281 (2010) 732.

[33] M. Aguiar, B. W. Kooi, J. Martins, N. Stollenwerk, Scaling of stochasticity in dengue hemorrhagic fever epidemics, Math. Model. Nat. Phenom. 7 (2012) 1–11.

[34] F. Rocha, M. Aguiar, Understanding the effect of vector dynamics in epidemic models using center manifold analysis, AIP Conference Proceedings 1479 (2012) 1–11.

[35] B. W. Kooi, N. Stollenwerk, M. Aguiar, Analysis of an asymmetric two-strain dengue model, Math Biosci 248 (2014) 128–39.

[36] M. Aguiar, R. Paul, A. Sakuntabhai, N. Stollenwerk, Are we modelling the correct dataset? minimizing false predictions for dengue fever in thailand, Epidemiol Infect 142 (2014) 2447–59.

[37] F. Rocha, L. Mateus, U. Skwara, M. Aguiar, N. Stollenwerk, Understanding dengue fever dynamics: a study of seasonality in vector-borne disease models, International Journal of Computer Mathematics 93 (2016) 1405–1422.

[38] N. Stollenwerk, P. F. Sommer, B. W. Kooi, L. Mateus, P. Ghaffari, M. Aguiar, Hopf and torus bifurcations, torus destruction and chaos in population biology, Ecological Complexity 30 (2017) 91–99.

[39] P. Rashkov, E. Venturino, M. Aguiar, N. Stollenwerk, B. W. Kooi, On the role of vector modeling in a minimalistic epidemic model, Mathematical Biosciences and Engineering 16(5) (2019) 4314–4338.

[40] P. Rashkov, B. W. Kooi, Complexity of host-vector dynamics in a two-strain dengue model, Journal of Biological Dynamics 15 (2021) 35–72. PMID: 33357025.

[41] E. Shim, Optimal dengue vaccination strategies of seropositive individuals, Mathematical Biosciences and Engineering 16 (2019) 1171–1189.

[42] W. Bock, Y. Jayathunga, Optimal control of a multi-patch Dengue model under the influence of Wolbachia bacterium, Mathematical Biosciences 315 (2019) 108219.

[43] J. K. Ghosh, U. Ghosh, S. Sarkar, Qualitative Analysis and Optimal Control of a Two-Strain Dengue Model with its Co-infections, International Journal of Applied and Computational Mathematics 6 (2020) 161.

[44] L. Xue, H. Zhang, W. Sun, C. Scoglio, Transmission dynamics of multi-strain dengue virus with cross-immunity, Applied Mathematics and Computation 392 (2021) 125742.

[45] J. K. K. Asamoah, E. Yankson, E. Okyere, G.-Q. Sun, Z. Jin, R. Jan, Fatmawati, Optimal control and cost-effectiveness analysis for dengue fever model with asymptomatic and partial immune individuals,, Results in Physics 31 (2021) 104919.

[46] V. Steindorf, A. K. Srivastav, N. Stollenwerk, B. W. Kooi, M. Aguiar, Modeling secondary infections with temporary immunity and disease enhancement factor: Mechanisms for complex dynamics in simple epidemiological models, Chaos, Solitons & Fractals 164 (2022) 112709.

[47] W. H. O. S. A. G. of Experts (SAGE), Revised sage recommendation on use of dengue vaccine, https://www.who.int/immunization/diseases/dengue/revised_SAGE_recommendations_dengue_vaccines_apr2018/en/, 2018.

[48] M. Aguiar, N. Stollenwerk, B. W. Kooi, Torus bifurcations, isolas and chaotic attractors in a simple dengue fever model with ade and temporary cross immunity, International Journal of Computer Mathematics 86 (2009) 1867–1877.

[49] M. Aguiar, N. Stollenwerk, B. W. Kooi, The stochastic multi-strain dengue model: Analysis of the dynamics, AIP Conference Proceedings 1389 (2011) 1224–1227.

[50] B. W. Kooi, M. Aguiar, N. Stollenwerk, Bifurcation analysis of a family of multi-strain epidemiology models, Journal of Computational and Applied Mathematics 252 (2013) 148–158.

[51] V. Duong, L. Lambrechts, R. E. Pau, et al., Asymptomatic humans transmit dengue virus to mosquitoes, Proc. Natl. Acad. Sci. 112 (2015) 14688–93.

[52] S. Marino, I. B. Hogue, C. J. Ray, D. E. Kirschner, A methodology for performing global uncertainty and sensitivity analysis in systems biology, J Theor Biol 254 (2008) 178–196.

[53] J. Wu, R. Dhingra, M. Gambhir, J. V. Remais, Sensitivity analysis of infectious disease models: methods, advances and their application., J R Soc Interface. 10 (2013) 20121018.

[54] F. Rocha, M. Aguiar, M. Souza, N. Stollenwerk, Time-scale separation and centre manifold analysis describing vector-borne disease dynamics, International Journal of Computer Mathematics 90 (2013) 2105–2125.

[55] C. for Disease Control, Prevention(CDC), https://www.cdc.gov/mosquitoes/mosquito-control/community/what-mosquito-control-programs-do.html, 2022.

[56] A. K. Srivastav, A. Kumar, P. K. Srivastava, M. Ghosh, Modeling and optimal control of dengue disease with screening and information, Eur. Phys. J. Plus 136 (2021) 1405–1422.

[57] M. R. Capeding, N. H. Tran, S. R. S. Hadinegoro, H. I. H. J. M. Ismail, T. Chotpitayasunondh, M. N. Chua, C. Q. L. et al., Clinical efficacy and safety of a novel tetravalent dengue vaccine in healthy children in Asia: a phase 3, randomised, observer-masked, placebo-controlled trial, Lancent 384 (2014) 1358–65.

[58] L. Villar, G. H. Dayan, J. L. Arredondo-García, et al., Efficacy of a tetravalent dengue vaccine in children in Latin America, New England Journal of Medicine 372 (2015) 113–123.

[59] X. Sáez-Llorens, V. Tricou, D. Yu, L. Rivera, J. Jimeno, A. C. Villarreal, E. Dato, S. Mazara, M. Vargas, M. Brose, M. Rauscher, S. Tuboi, A. Borkowski, D. Wallace, Immunogenicity and safety of one versus two doses of tetravalent dengue vaccine in healthy children aged 2-17 years in Asia and Latin America: 18-month interim data from a phase 2, randomised, placebo-controlled study, Lancet Infectious Disease 18 (2017) 1995–1206.

[60] E. López-Medina, S. Biswal, X. Saez-Llorens, C. Borja-Tabora, L. Bravo, C. Sirivichayakul, L. M. Vargas, M. T. Alera, H. Velásquez, H. Reynales, L. Rivera, V. Watanaveeradej, E. J. Rodriguez-Arenales, D. Yu, F. Espinoza, R. Dietze, L. K. Fernando, P. Wickramasinghe, J. Duarte Moreira, Edson, A. D. Fernando, D. Gunasekera, K. Luz, R. V. da Cunha, V. Tricou, M. Rauscher, M. Liu, I. LeFevre, D. Wallace, P. Kosalaraksa, T. S. G. Borkowski, Astrid, Efficacy of a Dengue Vaccine Candidate (TAK-003) in Healthy Children and Adolescents 2 Years after Vaccination, The Journal of Infectious Diseases 225 (2020) 1521–1532.

[61] S. B. Halstead, P. K. Russell, Protective and immunological behavior of chimeric yellow fever dengue vaccine, Vaccine 34 (2016) 1643–7.

[62] M. Aguiar, N. Stollenwerk, S. B. Halstead, The Impact of the Newly Licensed Dengue Vaccine in Endemic Countries, PLoS Neglected Tropical Diseases 12 (2016) e0005179.

[63] M. Aguiar, Dengue vaccination: A more ethical approach is needed., Lancet Infect. 391 (2018) 1769–1770.
[64] S. B. Halstead, L. C. Katzelnick, P. K. Russell, L. Markoff, M. Aguiar, L. R. Dans, , A. L. Dans, Ethics of a partially effective dengue vaccine: Lessons from the philippines., Vaccine 38 (2020) 5572–5576.
[65] W. H. O. S. A. G. of Experts (SAGE) on Immunization, Background paper on dengue vaccines prepared by the sage working group on dengue vaccines and the who secretariat, http://www.who.int/immunization/sage/meetings/2016/april/1_Background_Paper_Dengue_Vaccines_2016_03_17.pdf?ua=1, 2016.
[66] L. Coudeville, N. Baurin, E. Vergu, Estimation of parameters related to vaccine efficacy and dengue transmission from two large phase iii studies., Vaccine 34 (50) (2016) 6417–6425.
[67] S. updates, Sanofi updates information on dengue vaccine, https://www.sanofipasteur.com/-/media/Project/One-Sanofi-Web/Websites/Global/Sanofi-Pasteur-COM/Home/en/media-room/docs/PR_20171130_SanofiUpdatesInfoOnDengueVaccine_EN.pdf, 2017.
[68] S. Lenhart, J. T. Workman, Optimal control applied to biological models, Crc Press, 2007.
[69] L. S. Pontryagin, V. Boltyanskii, R. V. Gamkrelidze, E. F. Mishchenko, The mathematical theory of optimal processes, Wiley Press, 1962.
[70] P. van den Driessche, J. Watmough, Further Notes on the Basic Reproduction Number, Springer Berlin Heidelberg, Berlin, Heidelberg, 2008, pp. 159–178. doi:10.1007/978-3-540-78911-6_6.